Vegetation controls of water and energy balance of a drained peatland forest: Responses to alternative harvesting practices

Leppä, Kersti

2020-12

Leppä , K , Korkiakoski , M , Nieminen , M , Laiho , R , Hotanen , J-P , Kieloaho , A-J , Korpela , L , Laurila , T , Lohila , A K , Minkkinen , K , Mäkipää , R , Ojanen , P , Pearson , M , Penttilä , T , Tuovinen , J-P & Launiainen , S 2020 , ' Vegetation controls of water and energy balance of a drained peatland forest: Responses to alternative harvesting practices ' , Agricultural and Forest Meteorology , vol. 295 , 108198 . https://doi.org/10.1016/j.agrformet.2020.108198

http://hdl.handle.net/10138/320740
https://doi.org/10.1016/j.agrformet.2020.108198

Agricultural and Forest Meteorology 295 (2020) 108198

Contents lists available at ScienceDirect

Agricultural and Forest Meteorology

journal homepage: www.elsevier.com/locate/agrformet

Vegetation controls of water and energy balance of a drained peatland forest: Responses to alternative harvesting practices

Kersti Leppä[a,*], Mika Korkiakoski[b], Mika Nieminen[a], Raija Laiho[a], Juha-Pekka Hotanen[a], Antti-Jussi Kieloaho[a], Leila Korpela[a], Tuomas Laurila[b], Annalea Lohila[b,d], Kari Minkkinen[c], Raisa Mäkipää[a], Paavo Ojanen[c], Meeri Pearson[c], Timo Penttilä[a], Juha-Pekka Tuovinen[b], Samuli Launiainen[a]

[a] Natural Resources Institute Finland, Helsinki, Finland
[b] Finnish Meteorological Institute, Helsinki, Finland
[c] Department of Forest Sciences, University of Helsinki, Helsinki, Finland
[d] Institute for Atmospheric and Earth System Research/Physics (INAR), University of Helsinki, Finland

ARTICLE INFO

Keywords:
Eddy-covariance
Evapotranspiration
Partial harvesting
Peatland forestry
Soil-plant-atmosphere transfer model
Water table level

ABSTRACT

We quantified the response of peatland water table level (WTL) and energy fluxes to harvesting of a drained peatland forest. Two alternative harvests (clear-cut and partial harvest) were carried out in a mixed-species ditch-drained peatland forest in southern Finland, where water and energy balance components were monitored for six pre-treatment and three post-treatment growing seasons. To explore the responses caused by harvestings, we applied a mechanistic multi-layer soil-plant-atmosphere transfer model. At the clear-cut site, the mean growing season WTL rose by 0.18 ± 0.02 m (error estimate based on measurement uncertainty), while net radiation, and sensible and latent heat fluxes decreased after harvest. On the contrary, we observed only minor changes in energy fluxes and mean WTL (0.05 ± 0.03 m increase) at the partial harvest site, although as much as 70% of the stand basal area was removed and leaf-area index was reduced to half. The small changes were mainly explained by increased water use of spruce undergrowth and field layer vegetation, as well as increased forest floor evaporation. The rapid establishment of field layer vegetation had a significant role in energy balance recovery at the clear-cut site. At partial harvest, chlorophyll fluorescence measurements and model-data comparison suggested the shade-adapted spruce undergrowth was suffering from light stress during the first post-harvest growing season. We conclude that in addition to stand basal area, species composition and stand structure need to be considered when controlling WTL in peatland forests with partial harvesting. Our results have important implications on the operational use of continuous cover forestry on drained peatlands. A continuously maintained tree cover with significant evapotranspiration capacity could enable optimizing WTL from both tree growth and environmental perspectives.

1. Introduction

Water table level (WTL) is central for biogeochemical processes and resulting provisioning and regulatory ecosystem services of peatlands. WTL determines the depth of the oxic layer, which, together with the nutrient regime, controls vegetation composition and dynamics in pristine peatlands (Malhotra et al., 2016; Weltzin et al., 2003), as well as the productivity of forested (Hånell, 1988; Hökkä et al., 2008b; Préfontaine and Jutras, 2017) and agricultural peatlands (Berglund and Berglund, 2011; Musarika et al., 2017). WTL further affects peat decomposition and soil greenhouse gas emissions (Martikainen et al., 1993; Moore and Knowles, 1989; Ojanen et al., 2013, 2010; Ojanen and Minkkinen, 2019), and nutrient and carbon leaching to water courses (Kaila et al., 2014; Koskinen et al., 2011; Nieminen et al., 2015). Peatland water balance and WTL are driven by climatic forcing and site-specific factors including vegetation characteristics, soil properties and topography, as well as artificial drainage and changes in land-use and management (Holden, 2006; Holden et al., 2006; Waddington et al., 2015). It has been suggested that optimizing WTL to simultaneously support multiple ecosystem services can improve the sustainability of peatland use across boreal, temperate and tropical regions (Nieminen et al., 2018; Regina et al., 2015; Renger et al., 2002).

* Corresponding author. Latokartanonkaari 9, FI-00790 Helsinki, Finland.
E-mail address: kersti.leppa@luke.fi (K. Leppä).

https://doi.org/10.1016/j.agrformet.2020.108198
Received 27 April 2020; Received in revised form 17 September 2020; Accepted 17 September 2020
Available online 29 September 2020

Globally, about 15 million ha of peatlands have been drained for forestry since the early 1900s. Most of that area is in northern Europe. The peatland forests currently provide an important source of wood-based biomass; in Finland for instance, drained peatlands contribute by ca. 20% to the total annual stem volume increment (Päivänen and Hånell, 2012). In the Nordic countries, the prevailing management of peatland forests has been even-aged forestry with 60–100 year stand rotation, during which two or three thinnings are recommended (Kojola et al., 2004). As drainage ditches deteriorate over time, ditch cleaning is recommended every 20–40 years (Sikström and Hökkä, 2016). After clear-cutting, establishing the new tree generation is ensured by site preparation and regeneration by sowing, planting or through natural seeding. Many peatlands are potentially excellent forest soils when not excessively wet, due to the relatively high soil nitrogen content (Westman and Laiho, 2003). However, maintaining a ditch network means extra costs, and there are more environmental detriments involved in forestry on peat soils than on mineral soils.

Forest management on peatlands has impaired water quality and affected downstream aquatic habitats, mainly through erosion induced by ditch cleaning (Joensuu et al., 1999; Nieminen et al., 2010) and enhanced leaching of phosphorus, nitrogen, and dissolved organic carbon during high WTL periods after clear-cut (Kaila et al., 2015, 2014; Nieminen et al., 2015). In terms of peatland greenhouse gas balance, anoxic conditions after clear-cut increase soil methane emissions, while in mature, densely stocked stands greater peat aeration accelerates decomposition enhancing carbon dioxide (CO_2) and nitrous oxide emissions (Korkiakoski et al., 2019a; Ojanen et al., 2013, 2010). The latter being especially true for fertile drained peatland forests (Ojanen et al., 2010).

Recently, continuous cover forestry (CCF) has been proposed preferential to even-aged management from both environmental and economic perspectives (Juutinen et al., 2018; Nieminen et al., 2018; Tahvonen, 2016). CCF replaces clear-cuts by partial harvests, avoids site preparation and relies on natural regeneration (Pommerening and Murphy, 2004). In peatland forests that are often structurally heterogeneous even when managed according to the principles of even-aged management (Sarkkola et al., 2005, 2003), moving to CCF could be particularly feasible. By relying on natural regeneration, CCF would reduce the costs associated with regeneration by planting or sowing and soil preparation (Juutinen et al., 2018; Nieminen et al., 2018). Moreover, maintaining a continuous tree cover with significant evapotranspiration (ET) capacity could reduce the need for regular ditch cleanings and result in more stable WTL than in even-aged forests, which could be favorable from water quality and climatic perspectives (Nieminen et al., 2018). In the hydrological context, moving to CCF means a transition from ensuring satisfactory drainage by regular ditch cleanings towards relying on the ET capacity of the tree stand. This requires in-depth understanding on the water and energy balance of drained peatland forests which are linked through ET. Especially on how ET components, i.e. canopy interception evaporation, plant transpiration and forest floor evaporation, are affected by species water use traits, leaf-area index (LAI) and stand structure (Banerjee and Linn, 2018; Bowden and Bauerle, 2008; Launiainen et al., 2016), and how these are reflected in WTL.

Studies on boreal drained peatland forests show that mean growing season WTL correlates with stand volume (Ahti and Hökkä, 2006; Hökkä et al., 2008b, 2008a; Sarkkola et al., 2010), but that the shape and strength of this relationship is affected by climatic conditions, site type and drainage configuration (Hökkä et al., 2008a; Sarkkola et al., 2010). The relationship between WTL and stand volume is most pronounced in late summer, and has been attributed to high ET (Ahti, 1987, p. 198; Heikurainen, 1967; Sarkkola et al., 2013, 2010). Further, experimental studies show consistent increase in WTL by 0.2–0.4 m following clear-cut (Dubé et al., 1995; Heikurainen, 1967; Jutras and Plamondon, 2005; Sarkkola et al., 2013), indicating that ditch drainage is seldom sufficient to compensate for the lowered ET. However, the processes contributing to the recovery of WTL after clear-cut, and the impacts of partial harvests on peatland water and energy balance are not well described.

Partial harvest reduces stand volume and LAI, and alters the vertical foliage distribution and species composition, triggering changes in the coupled energy, water and carbon cycles. In a more open canopy, radiation, wind and vapor pressure deficit (VPD) increase in the lower canopy layers (Banerjee and Linn, 2018; Bladon et al., 2006; Launiainen et al., 2016; Vesala et al., 2005). As leaf photosynthetic CO_2 demand and stomatal conductance respond to these environmental variables (Katul et al., 2010; Launiainen et al., 2011), transpiration both at individual leaves and tree-level are likely to increase after partial harvest (Bladon et al., 2006; Bréda et al., 1995; Lagergren and Lindroth, 2004). At stand-scale, this is expected to partially compensate for the reduced LAI, as suggested by the studies from mineral soil sites showing that transpiration decreases proportionally less than LAI or basal area (Bréda et al., 1995; Gebhardt et al., 2014; Lagergren et al., 2008). This may be explained by changes in species composition (Bladon et al., 2006), adaptation to altered microclimatic conditions (Gebauer et al., 2011), or reduced resource competition (Bréda et al., 1995; Lagergren and Lindroth, 2004).

Trees affect site water balance also through interception evaporation, i.e. precipitation captured by the canopy and evaporated back to the atmosphere, and it has been suggested that stand interception scales with stand density (Mazza et al., 2011). After partial harvest, the understory receives more throughfall and light, and becomes dynamically more coupled with the atmosphere, enhancing transpiration of the undergrowth trees and the field layer vegetation, and evaporation from the forest floor (Boczoń et al., 2016; Simonin et al., 2007). Following disturbance and altered microclimate, the field layer vegetation often undergoes rapid changes in terms of species composition and coverage (Bergstedt and Milberg, 2001; Hamberg et al., 2019; Hannerz and Hånell, 1993; Mäkiranta et al., 2010). However, the role of field layer vegetation development after harvesting in peatland energy balance and WTL are poorly understood.

The overall objective of this study is to increase understanding on the role of vegetation on WTL, energy fluxes and water balance in boreal drained peatland forests. Such information is important for the proposed transition towards CCF and optimizing WTL for multiple ecosystem services on drained peatlands (Nieminen et al., 2018). Specifically, we address the following research questions:

1) How do growing season WTL and energy fluxes respond to clear-cut and partial harvest in a fertile boreal drained peatland forest?
2) What is the role of vegetation recovery in water and energy balances during post-treatment years?
3) How do stand structure, species composition and inter-annual meteorological variability affect WTL and ET components?

To find answers to these questions, a field experiment with two alternative harvesting treatments was conducted in a fertile, mixed-species peatland forest in southern Finland. ET and energy fluxes were measured using eddy-covariance (EC) technique for six pre-treatment and three post-treatment growing seasons, accompanied by systematic WTL monitoring, meteorological measurements and vegetation surveys. As field experiments alone do not necessarily reveal the causes of observed changes, a multi-layer soil-plant-atmosphere transfer model (Launiainen et al., 2015) was applied. The model was first run for the pre-treatment period, and then to used explain the underlying mechanisms of altered energy fluxes and WTL following harvesting. Finally, the model was used to disentangle the roles of vegetation and meteorological conditions on ET and WTL, to explore the hypothesis that species composition and structure of remaining vegetation are key factors in controlling WTL in peatland forests after partial harvest.

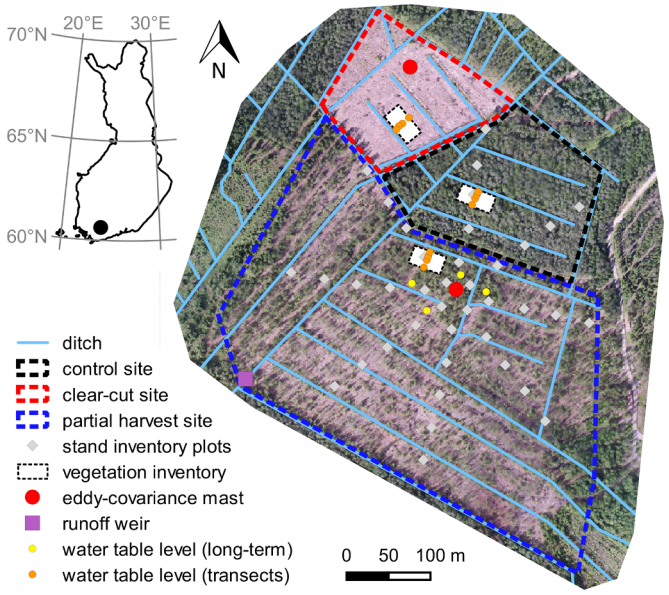

Fig. 1. Location of the Lettosuo site (60°38′N, 23°57′E) in southern Finland and an aerial photograph of the site after harvesting. The graphics depict the ditches and the monitoring setup.

2. Material and methods

2.1. Study site

The Lettosuo site is a fertile peatland forest located in southern Finland (60°38′N, 23°57′E; Fig. 1). The site was originally a mesotrophic birch-pine fen, drained with widely spaced, manually dug ditches probably during the 1930s, and later in 1969 more effectively with ditches spaced ca. 45 m apart and ca. 1 m deep. The area is flat, with an average slope of 0.2°. The peat layer thickness varies within 1.5–2.5 m, and the average carbon-nitrogen (C:N) ratio is 27, which is typical for sites with mesotrophic fen history. Before the harvest treatments, the two-storied tree stand consisted of a mixture of Scots pine (*Pinus sylvestris*, stem volume 180 m^3 ha^{-1}) and pubescent birch (*Betula pubescens*, 48 m^3 ha^{-1}) in the dominant layer, with a dense undergrowth of Norway spruce (*Picea abies*, 34 m^3 ha^{-1}). Field layer vegetation was patchy, featuring mostly herbs (*Dryopteris carthusiana, Trientalis europaea*) and dwarf shrubs (*Vaccinium myrtillus*). The forest floor was covered by litter and a patchy moss layer dominated by feather mosses (*Pleurozium schreberi* and *Dicranum polysetum*).

The long-term (1981–2010) annual mean temperature and precipitation at the nearby weather station were 4.6 °C and 627 mm, respectively (Pirinen et al., 2012). Snow typically covers the ground from December to April. Monitoring of the site started in the autumn of 2009 when an EC mast was installed in the center of the site to measure energy and CO_2 fluxes above the forest canopy (Fig. 1). In March 2016, two harvesting treatments were carried out, creating three parallel sites (Fig. 1): an area of 2.3 ha was clear-cut, 13 ha were partially harvested by removing the dominant pine trees, and the remaining 3.1 ha were left intact as a control. At the clear-cut site, a second EC mast was established in April 2016, the soil was prepared by mounding (see e.g. Nieminen, 2003) in August 2016, and spruce seedlings were planted in 2017.

2.2. Soil-plant-atmosphere transfer model

The soil-plant-atmosphere transfer model pyAPES (Launiainen et al., 2015) was used to analyze the observed changes in water and energy fluxes following the harvesting treatments, and to disentangle the relative roles of vegetation vs. meteorological controls on peatland water balance. pyAPES simulates water, energy and CO_2 fluxes in a forest ecosystem in a one-dimensional column. The forest ecosystem is described by a multi-species tree stand, field layer vegetation, a forest floor covered by mosses or litter, and an underlying soil profile. As forcing variables, the model uses time-averaged (here half-hourly) meteorological variables at a reference level above the canopy. Forcing variables are precipitation, downwelling longwave radiation, direct and diffuse photosynthetically active and near-infrared radiation (PAR and NIR), wind speed, atmospheric pressure, air temperature, and mixing ratios of H_2O and CO_2.

Canopy structure is described by a vertical leaf area density (LAD, m^2 m^{-3}) distribution that forms a layered porous medium, which is used to solve the transfer and absorption of shortwave and longwave radiation (Zhao and Qualls, 2006, 2005), and the turbulent transport of scalars (air temperature, H_2O, CO_2) and momentum within the canopy. The turbulent transport in the canopy air space and resulting vertical gradients of wind speed, air temperature, H_2O, CO_2 are modelled using standard first order closure schemes (Launiainen et al., 2015). Partitioning of precipitation between interception and throughfall, as well as the energy balance of wet leaves are solved in the canopy layers following Watanabe and Mizutani (1996).

The canopy LAD distribution is the superposition of the LAD distributions of individual plant types (here the tree species pine, birch and spruce and the field layer vegetation). Each plant type is characterized by its unique structural (LAD, leaf size etc.) and physiological properties, including photosynthetic parameters, water use traits and phenology. Leaf gas and energy exchange is solved separately for sunlit and shaded leaves of each plant type and canopy layer. Well-established solutions of coupled photosynthesis–stomatal conductance and leaf energy balance are applied (Farquhar et al., 1980; Medlyn et al., 2011) iteratively with the solution of canopy air-space scalar gradients and longwave radiation. During times with no snowpack, the forest floor is described as a mosaic of moss and litter. Both the moss and litter compartments are solved for water and energy balance and CO_2 exchange (Kieloaho and Launianen, 2018; Launiainen et al., 2015). Snow accumulation and melt is described here with a simple temperature-based approach and parameterized as in Launiainen et al. (2019).

Vertical water flow in the soil is solved using Richards' equation and the van Genuchten scheme for water retention and unsaturated hydraulic conductivity following van Dam and Feddes (2000). Soil heat flow is computed based on heat conduction in the soil column. Heat flow in the soil is affected by freezing and thawing processes, calculated based on a freezing curve (e.g., Koivusalo et al., 2001). The lateral ditch drainage out of the soil column follows Hooghoudt's (1940) equation. We described macropore bypass flow by transporting 70% of the infiltrated water directly to the topmost water-saturated soil layer. This reproduced well the observed patterns in WTL also after strong infiltration events through otherwise poorly conductive dry peat layers during periods of deep WTL.

The model was first applied to the pre-treatment period (September 2009 to March 2016) to explore whether it could adequately reproduce the observed energy and water balances. Thereafter (March 2016 to December 2018), the model was applied to the three parallel sites. The model was forced, parameterized, and evaluated using measurement data described in Section 2.3. Parameters affected by the treatments include tree species' LAD distributions and LAI, field layer LAI, and forest floor coverage by moss and litter. Other model parameters, largely based on earlier literature, can be found in Tables S1 and S2. In the model runs, we divided the canopy into 100 canopy layers extending to the height of 25 m, and a 2 m deep soil profile with layer thickness ranging from 0.01 m at the soil surface to 0.1 m in deeper parts.

2.3. Measurements and data processing

2.3.1. Vegetation and peat characteristics

Tree stands were measured in November 2014 before harvest and in

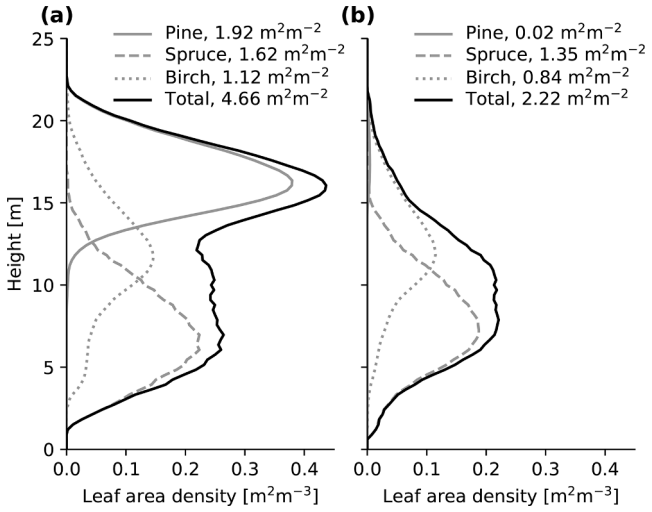

Fig. 2. Leaf area density distributions and leaf area indices of tree species: (a) before harvest in 2014, and (b) after partial harvest in 2016.

May 2016 after harvest on altogether 39 circular stand inventory plots. They were located systematically on eight radial transects extending 160–200 m from the central EC mast and covering an area of 4000 m^2 in total (Fig. 1). Tree species were identified and stem diameter at the height of 1.3 m (DBH) was recorded for all trees with DBH > 25 mm. Additionally, an earlier inventory of the same plots was carried out in 2009 to measure tree heights and crown lengths of sample trees. These data consisted of 57 pine, 40 spruce, and 37 birch trees distributed evenly on the inventory plots and covering the entire DBH ranges of each species. The partial harvest reduced the canopy density considerably; the number of stems decreased from 2100 ha^{-1} to about 1100 ha^{-1} and basal area from 32 m^2 ha^{-1} to 10 m^2 ha^{-1}. Pine, spruce and birch accounted for 60%, 20% and 20% of basal area before harvest, and 2%, 51% and 47% after harvest, respectively. The stand inventory data were used to derive vertical LAD distributions for each tree species and tree stand LAI during pre- and post-treatment conditions (Fig. 2; details in Appendix A).

To evaluate the physiological status of the foliage of remaining spruce undergrowth after partial harvest, chlorophyll fluorescence, more precisely the ratio of variable fluorescence to maximal fluorescence (Fv/Fm), was measured. Fv/Fm describes the maximum efficiency of Photosystem II (PS II) (Murchie and Lawson, 2013). Measurements were taken from current-year and one-year-old needles of 70 spruce trees ranging from 1 to 16 m in height: 50 in different parts of the partial harvest area and 20 in the control area. Altogether 19 measurement times during the growing seasons of 2016 and 2017 were chosen to follow the post-harvest dynamics of Fv/Fm in the two parallel sites. Each time, one lateral shoot from the upper third of the live canopy per tree was detached, placed in a plastic bag, and stored cool before the measurement (max. 3 h). In the laboratory, the target needles (the two age classes separately for each shoot) were first dark adapted for 30 min using PPEA/LC dark adaptation leafclips (Hansatech Instruments, King's Lynn, Norfolk, UK). Then, measurements were done with a Pocket PEA continuous excitation chlorophyll fluorimeter (Hansatech Instruments; measure duration 1 s, illumination 3500 micromoles).

The understory vegetation was monitored by assessing the projection coverage of field layer species (dwarf shrubs, herbs, graminoids, and tree and shrub seedlings and saplings up to 0.5 m height) and that of moss species and litter on the forest floor. The species names used for vascular plants and mosses follow the nomenclatures of Hämet-Ahti et al. (1998) and Ulvinen et al. (2002), respectively. Inventories were carried out in the tree stand inventory plots in 2009, 2017, and 2018 (only in partial harvest site in 2018), as well as in a systematic grid of 32 vegetation plots in each parallel site. The latter plots were located around the WTL transects (Fig. 1) and were mapped for vegetation in 2015, 2017, and 2018 (only the harvested sites in 2018). The moss projection coverage on the forest floor and the field layer vegetation LAI were derived from these data for each treatment (Table 1; details in Appendix A).

Table 1
Leaf area indices (LAI) and moss coverage at different treatments[a].

	Pre-treatment / Control	Partial harvest	Clear-cut
Tree stand LAI (m^2 m^{-2})	4.66	2.22	0.0
Field layer LAI (m^2 m^{-2})	1.0	0.4[b]–1.2	0.3[b]–1.3
Moss projection coverage (%)	40	40	10

[a] The field layer LAI ranges for the harvested sites describe the development after harvest during 2016–2018.
[b] Estimated for 2016 assuming a similar change as observed between 2017 and 2018.

Table 2
Peat profile hydraulic characteristics.

Depth (m)	θ_s (m^3 m^{-3})	θ_r (m^3 m^{-3})	α_{vg} (m^{-1})	β_{vg} (–)	K_{Vsat} (m h^{-1})	K_{Hsat} (m h^{-1})
0–0.1	0.94	0.002	20.2	1.35	0.18	30 × K_{Vsat}
0.1–0.2	0.88	0.010	4.4	1.35	0.12	20 × K_{Vsat}
0.2–0.3	0.88	0.010	4.4	1.35	0.07	10 × K_{Vsat}
0.3–2.0	0.88	0.010	4.4	1.35	0.05–0.0004	K_{Vsat}

θ_s = soil porosity; θ_r = residual water content; α_{vg}, β_{vg} = van Genuchten water retention curve parameters;
K_{Vsat}, K_{Hsat} = saturated vertical and horizontal hydraulic conductivity.

To characterize the hydraulic properties of peat (Table 2), peat samples were collected from three locations. They were analyzed for peat type and degree of humification (von Post, 1922) for each 0.1 m layer extending from soil surface to the depth of 0.5 m. The top layer consisted of organic matter accumulated after drainage ("raw humus") and the lower layers were *Carex* peat with the degree of decomposition varying from 4 to 6 (von Post scale). Water retention characteristics and hydraulic conductivities of the peat layers were defined based on Päivänen (1973): The soil layers below 0.1 m from the soil surface were described with water retention parameters fitted to all the *Carex* peat data presented by Päivänen (1973), while the water retention parameters of the topmost 0.1 m layer were set based on the *Carex* sample with the poorest water retention capacity. Saturated hydraulic conductivity for each 0.1 m layer was defined in relation to depth with the functions presented for *Carex* peat. The horizontal hydraulic conductivities of the top 0.3 m of the peat profile were further adjusted by manual calibration against WTL and runoff measurements during the pre-treatment period.

2.3.2. Meteorological conditions

Meteorological data were recorded as 30 min averages. The utilized data included air temperature (HMP45D, Vaisala Corporation), relative humidity (HMP45D, Vaisala Corporation), atmospheric pressure (PMT16A, Vaisala Corporation), incoming global radiation (R_g; Pyranometer CMP3, Kipp & Zonen, Delft, The Netherlands), incoming PAR (PQS1 PAR Quantum sensor, Kipp & Zonen), wind speed and friction velocity (METEK USA-1, METEK GMbH) measured at the central EC mast at 25.5 m. In addition, precipitation (Casella Ltd Par NO 10000E-04) was measured at 6 m. Meteorological data from three nearby weather stations (Jokioinen (60°48′N, 23°30′E), Somero (60°39′N, 23°48′E), and Salo Kiikala (60°27′N, 23°39′E)), operated by the Finnish Meteorological Institute, were used to complete the wintertime precipitation data and to fill the gaps in the on-site

Table 3
Coverage of EC measurements and energy balance closure during May–September.

	Pre-treatment						Partial harvest			Clear-cut		
	2010	2011	2012	2013	2014	2015	2016	2017	2018	2016	2017	2018
Coverage of H [%]	55.4	60.2	73.7	66.7	54.0	68.9	22.7	17.4	16.1	28.1	35.4	22.3
Coverage of LE [%]	48.3	52.1	63.4	53.2	42.3	58.1	22.1	16.0	15.0	28.0	35.2	22.3
Energy balance closure [-][a]	0.99	0.93	1.03	0.93	0.97	0.99	1.00	1.03	1.14	0.82	0.82	0.79

[a] slope of the linear least-squares regression of half-hourly (H + LE) against (R_n–G) H = sensible heat flux; LE = latent heat flux; R_n = net radiation; G = ground heat flux.

meteorological time series.

Downwelling longwave radiation (LW_d) was recorded since 2013 at the Tervalamminsuo mire (CGR4 Pyrgeometer, Kipp & Zonen), ca. 1 km northeast of the study site. Before 2013 and for gaps in data, LW_d was estimated from air temperature and atmospheric emissivity with cloud-cover fraction derived from R_g following Song et al. (2009). The method proposed by Song et al. (2009) was also applied for decomposing measured R_g into its direct and diffuse components. A constant CO_2 mixing ratio of 400 ppm was used as model input.

2.3.3. Energy balance components and gross primary production

The two EC setups were used to measure vertical ecosystem–atmosphere fluxes of CO_2, sensible heat (H) and latent heat (LE) (Fig. 1). The 25.5 m high central EC mast provided data for the pre-treatment period (2010–2015) and for the partial harvest thereafter (Mar 2016–Dec 2018). The lower 2.75 m EC mast provided data for the clear-cut site (Apr 2016–Dec 2018) (Korkiakoski et al., 2019a). The study design did not enable detecting turbulent fluxes (CO_2, H and LE) with EC from the control area after harvesting. The measurement setup also included net radiation (R_n) at both EC stations (Nr-lite net radiometer, Kipp & Zonen), as well as reflected shortwave radiation at the central EC mast (Pyranometer CMP3, Kipp & Zonen). Ground heat flux (G) was measured at each parallel site from one location at a depth of 0.07 m (HFP01, Hukseflux Thermal Sensors B.V., Delft, the Netherlands). The relation between energy fluxes can be expressed as the surface energy balance:

$$\underbrace{(1-\alpha)R_g + \varepsilon_s(LW_d - \sigma T_s^4)}_{R_n} = H + LE + G + \frac{dF}{dt} \quad (1)$$

where α is broadband albedo, ε_s is emissivity, σ is the Stefan-Boltzman constant, T_s is effective surface temperature, and dF/dt is the change in energy storage within the aboveground vegetation, air volume, and topsoil above the depth of G measurements.

The EC system setup and data processing for the clear-cut site was described in detail by Korkiakoski et al. (2019a). This system included a three-axis sonic anemometer (uSonic-3 Scientific, METEK, Elmshorn, Germany) for wind speed and air temperature and a closed-path infrared gas analyzer (LI-7000, LI-COR Biosciences, Lincoln, NE, USA) for CO_2 and H_2O mixing ratios. The system at the central EC mast had the same gas analyzer model, but a different sonic anemometer (METEK USA-1, METEK).

Half-hourly turbulent fluxes of H and LE were calculated from the EC data and filtered using standard methods (Aubinet et al., 2012). The 10 Hz raw data were block-averaged, and a double rotation of the coordinate system was applied (McMillen, 1988). The time lags between anemometer and gas analyzer were determined by a cross correlation analysis. CO_2 fluxes were calculated from the dry mixing ratios to eliminate water vapor fluctuations (Webb et al., 1980). The transfer function method of Moore (1986) with an empirically determined time response of each measurement system was used to compensate for the attenuation of high-frequency fluctuations (Korkiakoski et al., 2019a). The flux data from both sites were screened according to the following criteria: relative stationarity (Foken and Wichura, 1996) < 100%, internal analyzer pressure > 60 kPa (central mast) or > 75 kPa (clear-cut), CO_2 mixing ratio > 350 ppm, wind direction within 90–300° (central mast after partial harvest) or 80–315° (clear-cut), and number of spikes in the vertical wind speed and CO_2 concentration data < 150 of 18,000. Periods of weak turbulence were discarded by applying a friction velocity limits of 0.125 m s^{-1} at the clear-cut and 0.225 m s^{-1} at the central mast. The flux footprints were calculated using the model by Kormann and Meixner (2001) and input data measured with the sonic anemometer. The footprint accumulated within the target area was required to exceed 75% to ensure the measured flux originated predominantly from the target site. At the central EC mast in January 2012, heating of the anemometer was switched on, which is known to affect especially fluxes of H (Goodrich et al., 2016). Here, the effect seemed to be a rather constant overestimation of ca. 33 W m^{-2} and thus, after January 2012, H was corrected accordingly.

Data coverage of the EC measurements was considerably lower for the post- than the pre-treatment years (Table 3, see Figs. S1–S6 in the Supplement for full visualization of data), because of occasional instrument failures and unavoidable wind direction filtering. The coverage was higher during daytime (zenith angle < 90°) than nighttime: 65–74% vs. 27–40% during pre-treatment, 23–25% vs. 6% at partial harvest, and 35% vs. 15% at clear-cut, respectively. 78%, 42% and 66% of the missing values occurred during gaps shorter than one day long in the pre-treatment, partial harvest and clear-cut data, respectively. Each treatment had a few gaps longer than 14 days, the longest (38 days) occurring in 2018 at the partial harvest.

In the analyses of EC data, we primarily use measured half-hourly LE and H fluxes but also daily fluxes (for days with >50% of measurements available) and estimates of cumulative ET. For the latter two purposes, LE and H fluxes were gap-filled using the REddyProc online tool (Wutzler et al., 2018). It applies marginal distribution sampling for gap-filling, which consists of a combination of look-up tables (based on global radiation, air temperature and vapor pressure deficit) and mean diurnal variation of fluxes. For seasonal ET, we additionally present the uncertainty of the estimates that is based on the variability of the half-hourly fluxes associated with the bins used for gap-filling (Wutzler et al., 2018). Uncertainties were aggregated to seasonal values accounting for correlations between records.

The energy balance closure in May–September (Table 3) was evaluated as the slope of the linear least-squares regression of half-hourly H + LE against R_n–G without considering storage terms (Leuning et al., 2012). At the central EC mast, energy balance closure was close to 1.0 except for the year 2018 (1.14), while at the clear-cut site, it was about 0.8.

In addition to energy fluxes (R_n, H, LE, and G), we also used gross primary production (GPP) to assess the model performance during the pre-treatment period and the role of vegetation recovery after partial harvest and clear-cut. Half-hourly GPP values were estimated from the measured CO_2 fluxes by partitioning them using the environmental response functions and procedures described by Minkkinen et al. (2018) and Korkiakoski et al. (2019a). In short, the measured CO_2 flux, i.e. net ecosystem exchange, was assumed to be the sum of ecosystem respiration and GPP, which were modelled as a function of air temperature and photosynthetically active radiation, respectively. In the model-data comparison of half-hourly turbulent fluxes, we excluded time periods with > 5 mm of rainfall within the last 24 h to avoid the

uncertainties introduced by wet-canopy conditions to EC measurements (Kang et al., 2018; van Dijk et al., 2015).

2.3.4. WTL and water balance components

The distance of the water table from the soil surface, WTL, was monitored since May 2010 with four automatic loggers (TruTrack WT-HR, Intech Instruments Ltd, Auckland, New Zealand) located around the central EC mast (Fig. 1). Additionally, four loggers (Odyssey Capacitance Water Level Logger, Dataflow Systems Limited, Christchurch, New Zealand) were installed on each site in December 2014 or July 2015 (clear-cut site). The four loggers were installed on transects running from the mid-strip to ditch (Fig. 1). All loggers recorded WTL at an hourly interval. The paired catchment approach (e.g., Kaila et al., 2014) was used to produce post-treatment WTL data that were comparable to the pre-treatment data (details in Appendix B).

Discharge was measured at an hourly interval since March 2012 using a V notch weir (90°) and a capacitance water level logger (TruTrack WT-HR). The weir was located at the southwest end of the area (Fig. 1). The water level data was calibrated against manual measurements taken at regular intervals, and discharge was calculated using the stage-discharge relationship. The weir design limited discharge measurements to 60 l s^{-1}, corresponding to a runoff of 1.3 mm h^{-1}. For the rare cases of higher discharge, this maximum value was applied. The discharge was converted to runoff using the estimated weir catchment area of 17.1 ha.

To calculate the May–September water balance during the pre-treatment period, measured WTLs were converted into changes in soil water storage (dS/dt) using the hydraulic characteristics defined in Table 2 and assuming that soil water in unsaturated peat profile is in hydraulic equilibrium. The resulting change in soil water storage was compared to precipitation (P), runoff (Q) and EC-based ET as defined by the water balance equation:

$$\frac{dS}{dt} = P - (ET + Q). \quad (2)$$

3. Results and discussion

3.1. Meteorological conditions

The meteorological conditions during the growing seasons of 2010–2018 varied considerably (Table 4). The third post-treatment year 2018 was in many ways extreme; it had the highest mean air temperature, VPD and R_g, resulting in largest equilibrium evaporation (ET_{eq}; calculated following McNaughton and Jarvis (1983)). Precipitation during May–September was also the lowest in 2018. The year 2010 had the highest pre-treatment ET_{eq}, and the year 2012 the lowest. The summer of 2014 was the rainiest (411 mm), while 2017 was the coldest and most humid growing season.

Table 4
Meteorological characteristics in May–September during 2010–2018[a].

Period	Pre-treatment						Post-treatment		
Year	2010	2011	2012	2013	2014	2015	2016	2017	2018
T_{air} [°C]	14.5	14.4	12.7	14.3	13.6	12.7	14.1	12.1	**15.5**
VPD [kPa]	0.53	0.45	0.38	0.45	0.43	0.38	0.43	0.37	**0.65**
R_g [W m^{-2}]	182	179	176	182	179	179	178	181	**199**
P [mm]	306	376	324	245	**411**	285	315	290	212
ET_{eq} [mm][b]	348	337	314	341	332	320	329	318	**389**

[a] The minimum value is underlined and maximum value bolded for each variable.

[b] Calculated following McNaughton and Jarvis (1983) using net radiation $R_n = 0.67R_g - 21$ (see Fig. 7a)

T_{air} = air temperature; VPD = vapor pressure deficit; R_g = global radiation; P = precipitation; ET_{eq} = equilibrium evaporation.

3.2. Pre-treatment period and model validation

According to measurements, mid-growing season R_n was about 60% of R_g during the pre-treatment period (Fig. 3a). Partitioning of R_n into its components showed distinct seasonal patterns (Fig. 3a–d). The daily mean H peaked before mid-June, while LE reached its peak in July. G increased sharply after snowmelt in April–May and had a decreasing trend thereafter. The relation between H and LE is typically expressed as the Bowen ratio (β = H/LE), whose seasonal dynamics are shown in Fig. 3e. H dominated over LE until mid-June (β > 1), while the opposite was true thereafter. The Priestley-Taylor parameter (α_{pt} = ET/ET_{eq}; Fig. 3f) indicates that ET was close to ET_{eq} from mid-June to late August. The observed β and α_{pt} are in the range previously reported for boreal coniferous forests (Amiro, 2001; Launiainen et al., 2016). The seasonal patterns are in line with observations for boreal forests and managed peatland ecosystems (Alekseychik et al., 2018; Arneth et al., 2006; Launiainen, 2010), where stomatal control of LE and energy partitioning are affected by dormancy recovery in early growing season (Kolari et al., 2007; Launiainen, 2010).

The model reproduced the seasonal energy flux dynamics and the mean diel cycles reasonably well (Figs. 3 and 4). However, R_n was systematically overestimated during daytime (Fig. 4a) resulting in a ca. 20 W m^{-2} overestimation of daily averages (Fig. 3a). As the net shortwave radiation was well reproduced (Fig. 4b), the slight mismatch in R_n is most likely due to the longwave radiation balance, which may be attributed by the absence of downwelling longwave radiation measurements at the site (see Section 2.3.2). The lowest coefficient of determination (R^2 = 0.60) was between the modelled and measured LE (Fig. 4d). This was likely caused by the presence of interception evaporation events, which cause high peaks in the modelled LE that are difficult to capture on a half-hourly time scale because of uncertainties in precipitation input and in EC measurements during wet-canopy conditions (Kang et al., 2018; van Dijk et al., 2015). The comparison already excluded time periods with > 5 mm of rainfall within the last 24 h but limiting the data even further to time periods with no rainfall within the last 24 h, improved the fit to R^2 = 0.68. The additional slight mismatch in the diel cycles of H, LE and GPP (Fig. 4c, d and f) may be related to the inertia in the response of stomatal control to the surrounding microclimate, which is not accounted for in the coupled leaf-scale photosynthesis-stomatal control model applied in pyAPES.

ET was the dominant component of the May–September water balance, exceeding even precipitation during all growing seasons except 2011 and 2014 (Fig. 5a). Over the growing season, the measured and modelled ET were 85–108% and 96–104% of ET_{eq} (Table 4), respectively. This is typical for boreal forests on both peat and mineral soils at similar latitudes, where ET is commonly reported to exceed growing season precipitation (Grelle et al., 1997; Launiainen, 2010; Sarkkola et al., 2013). Since 2012, when runoff data were available from the site, water balance was closed reasonably well (–11%…+7%) by the measurements (Fig. 5a). The presented water balance components are expected to close the water balance as we only consider the snow-free growing season. The most significant storage delaying water flow through the system during this time is the soil water storage, which was here computed from WTL based on assumptions presented in Section 2.3.4. Both the EC measurements and model showed highest ET in 2010 (Fig. 5a–b); this was the warmest and driest summer during the pre-treatment period (Table 4). On the other hand, the most humid and coldest summers (2012 and 2015) produced the lowest modelled ET, while the lowest measured ET occurred during the rainiest summer (2014). This difference can be caused by underestimated EC-based ET during wet-canopy conditions when evaporation of intercepted rainfall is significant (Kang et al., 2018; van Dijk et al., 2015).

According to the modeling, total transpiration was on average 64% of growing season ET (Fig. 5b), and tree stand transpiration covered 59% of ET. This agrees with earlier findings from boreal forests that show tree stand transpiration is 39–48% of ET in more northern

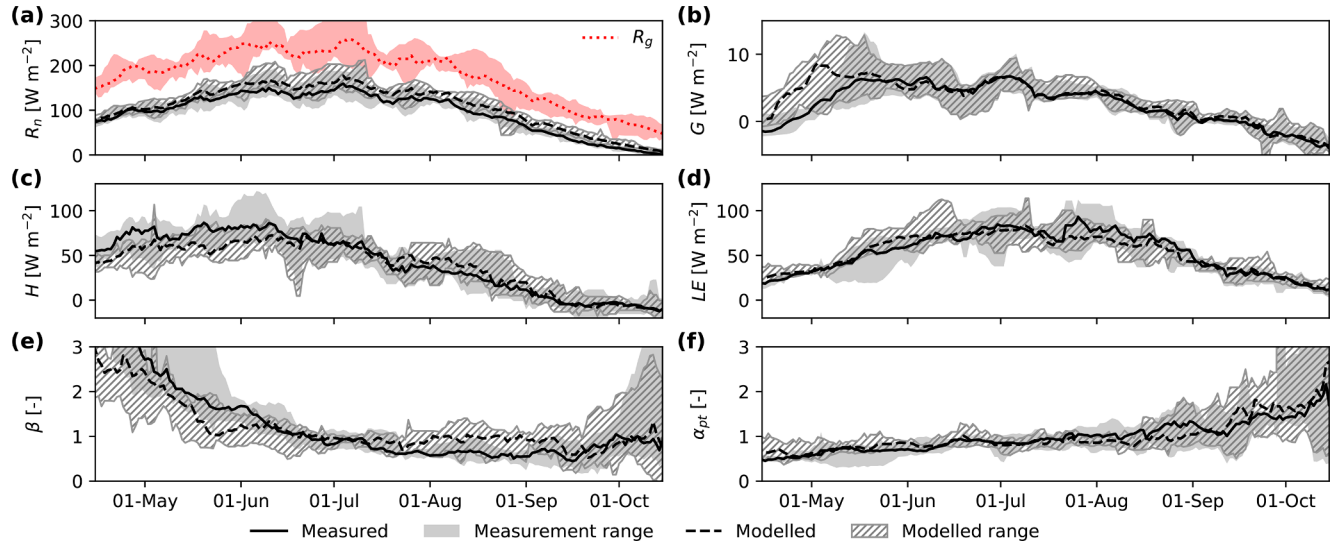

Fig. 3. Seasonal dynamics of variables characterizing the surface energy balance during the pre-treatment period 2010–2015: (a) net raditation, R_n, and global raditaion, R_g; (b) ground heat flux, G; (c) sensible heat flux, H; (d) latent heat flux, LE; (e) Bowen ratio, β; (f) Priestley-Taylor parameter, α_{pt}. Shaded areas show the range of yearly 14-day rolling means and the lines show the median values. The days with more than 50% of gap-filling and with > 5.0 mm of rainfall are excluded. Bowen ratio only includes periods when zenith angle was < 90°.

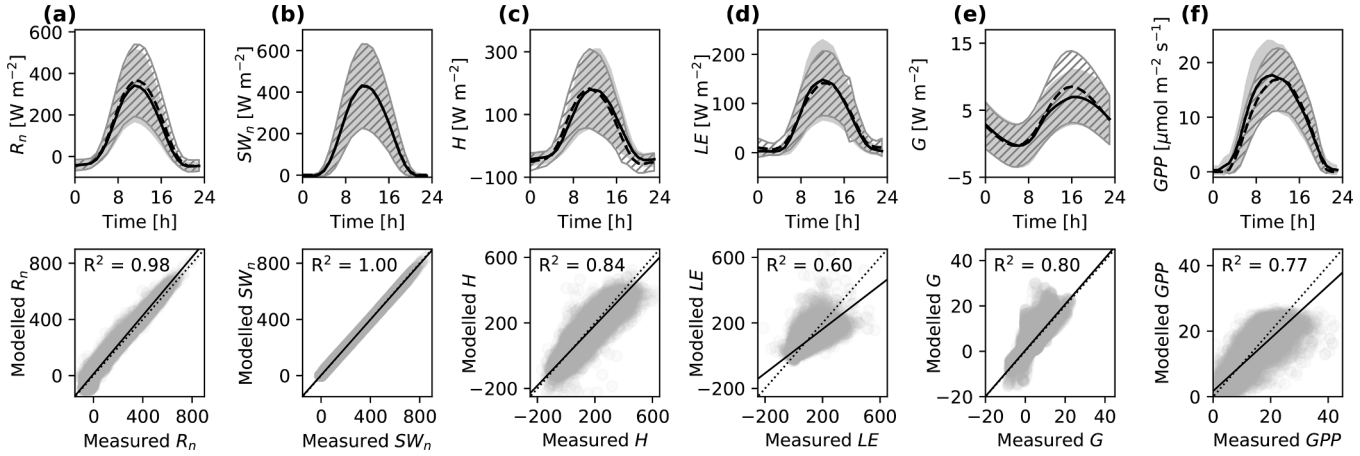

Fig. 4. Mean diel cycles of measured (solid line ± standard deviation as gray shade) and modelled (dashed line ± standard deviation as hatched lines) fluxes, and scatter plots of modelled vs. measured fluxes: (a) net radiation, R_n; (b) net shortwave radiation, SW_n; (c) sensible heat flux, H; (d) latent heat flux, LE; (e) ground heat flux, G; and (f) gross primary production, GPP. Plots include data from May–September, excluding periods with > 5.0 mm of rainfall within the past 24 h. Linear least-squares regressions are fitted to the half-hourly data (black line), 1:1 line shown as dotted, and R^2 denotes the coefficient of determination.

locations (Kozii et al., 2019; Sarkkola et al., 2013) and 65% in a more southern location (Grelle et al., 1997) compared to the location of Lettosuo. The model suggested that transpiration by the dominant pines was 47% and by birches 27% of total transpiration. The undergrowth spruces with just 15% smaller LAI than pine contributed only by 17% and field layer vegetation by 9%. This suggests that suppressed spruces and field layer vegetation have a minor role in a mature forest, but may have potential to increase their transpiration when the canopy opens up, as reported for undergrowth spruces by Lagergren and Lindroth (2004) following thinning.

The measured WTL ranged from −0.1 m during spring down to −0.7– −0.5 m in late summer (Fig. 5c). Average WTL in August was −0.54 m. This is in line with late summer WTL measured in managed peatland forest in southern Finland with tree stand volumes exceeding 200 m^3 ha^{-1} (Sarkkola et al., 2010) as in Lettosuo. The model reproduced the measured WTL with reasonable accuracy (Fig. 5c); the mean absolute error during May–September ranged from 0.03 to 0.09 m depending on the year. Overall, the comparisons between model predictions and measurement-based observations, and the outcomes being well in line with earlier studies in boreal forests, suggest that the model can be used to support the evaluation of harvest-induced effects.

3.3. Responses to harvesting

3.3.1. Observed WTL and ET

After harvesting, the largest WTL differences between the sites occurred during June–September while the differences were the smallest during the snowmelt period in April (Fig. 6). At the clear-cut site, WTL was up to 0.45 m higher compared to the control site. At the partial harvest site, the WTL rise was never more than 0.15 m, even though the partial harvest reduced the basal area by 70% and LAI by 50%. The smallest WTL differences between treatments were observed during the coldest and most humid growing season 2017. The exceptionally warm and dry 2018 yielded the largest differences, as well as the lowest WTL observed during the whole study period 2010–2018 (Figs. 5c and 6a). Compared to the control site, the average WTL rise for May–September during the post-treatment period (2016–2018) was 0.05 ± 0.03 m and 0.18 ± 0.02 m at the partial harvest and clear-cut sites, respectively

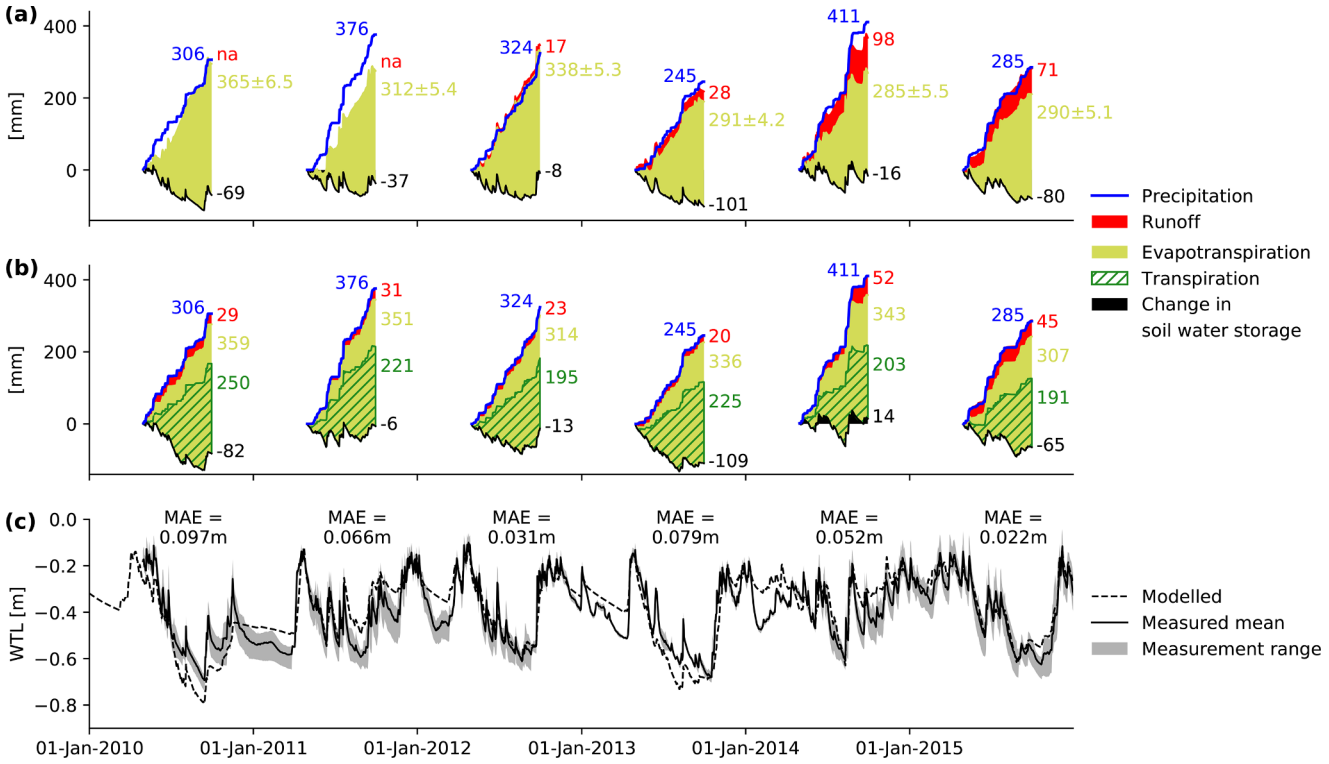

Fig. 5. Cumulative water balance during May–September for the pre-treatment period according to (a) measurements, and (b) model results; and (c) comparison of measured and modelled daily water table level (WTL). Error estimates of seasonal evapotranspiration (a) are derived from eddy-covariance data processing (see Section 2.3.3.). MAE denotes the mean absolute error of the modelled WTL in May–September. na = not available.

(error estimate is the standard deviation derived from the WTL measurements).

Seasonal cumulative ET derived from the EC measurements suggested that ET was about 30% lower at the clear-cut than at the partial harvest in 2016 and 2018 (Table 5). In 2017, however, ET was about the same for both sites (Table 5), which is inconsistent with the WTL observations (Fig. 6). The uncertainty induced by gap-filling to seasonal ET due to the low coverage of EC measurements (Table 3) is likely causing this inconsistency. The larger ET uncertainty estimates during the post-treatment (Table 5) compared to pre-treatment (Fig. 5) indicate this to some extent, although the uncertainty caused by filling longer gaps is not included in the error estimates. Compared to the modelled ET of the non-harvested control stand, ET changes after both harvests were largest during the first post-treatment year 2016

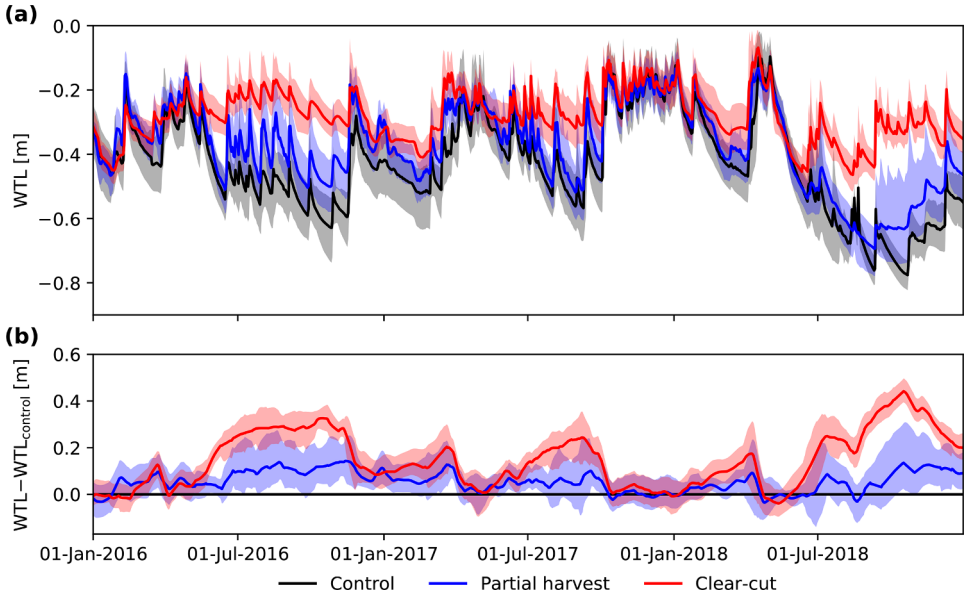

Fig. 6. (a) Post-treatment water table level (WTL) at each site, and (b) its difference compared to the control site as 14-day rolling mean. Lines and shaded areas indicate the mean and variability range of WTL measurements.

Table 5
Cumulative May–September evapotranspiration (ET) for the three post-treatment years. Error estimates are derived from eddy-covariance data processing (see Section 2.3.3.).

Year	ET [mm][a] 2016	2017	2018
Partial harvest[a]	264 ± 9.5	263 ± 6.4	388 ± 14.3
Clear-cut[a]	176 ± 8.0	261 ± 7.4	268 ± 8.1
Control[b]	320	294	380

[a] Based on eddy-covariance measurements.
[b] Modelled.

(Table 5). In 2018, ET at the partial harvest was similar to the control site but at the clear-cut it was still clearly lower.

The significant rise of WTL after clear-cut, that is commonly observed in peatlands (Dubé et al., 1995; Heikurainen, 1967; Jutras and Plamondon, 2005; Sarkkola et al., 2013), is addressed in operational peatland forestry by recommending ditch cleaning soon after clear-cut to maintain efficient drainage. The notably smaller WTL rise after partial harvest suggests ditch cleaning may not be necessary, which is a strong environmental and economical benefit compared to clear-cutting (Nieminen et al., 2018). The necessity of ditch cleaning in connection with partial harvest was questioned already by Päivänen and Sarkkola (2000) after their experiment where up to 30% of the stand volume was removed. Heikurainen and Päivänen (1970) reported that removing 60% of the volume of a Scots pine stand resulted in a WTL rise that was half of the response observed at a parallel clear-cut site. Here the observed WTL rise at the partial harvest was about 30% of that at the parallel clear-cut site (Fig. 6b), thus less drastic than the WTL rise after partial harvest observed by Heikurainen and Päivänen (1970).

3.3.2. Impacts on energy balance

Compared to the pre-treatment conditions, R_n decreased after both harvests (Figs. 7a and 8a). At the partial harvest site, the change was smaller than at the clear-cut but still statistically significant (evaluated as 95% confidence interval of regression curve coefficients in Fig. 7a). Two factors may jointly decrease R_n: (1) increased albedo and decreased absorption of solar radiation and (2) increased emittance of longwave radiation as a result of increased surface temperature (see Eq. (1)). Ecosystem-scale albedo, computed from the reflected vs. incoming R_g measured at the central EC mast, indicated that mean growing season albedo increased from 0.09 to 0.12 after partial harvest. The increase in albedo with decreasing LAI is in line with what has been observed across boreal coniferous stands (Kuusinen et al., 2014; Lukeš et al., 2013). Thus, about half of the decrease in R_n after partial harvest may be attributed to albedo changes. The albedo was not measured at the clear-cut site, but the decrease in R_n there should be affected both by increased albedo and increased surface temperature (Mamkin et al., 2019; McCaughey, 1981).

Both H and LE were significantly reduced after the clear-cut (Figs. 7b–c and 8b–c), as could be expected based on the results of earlier studies (Amiro, 2001; Mamkin et al., 2019; Rannik et al., 2002). Moreover, their relationship with R_g became more linear compared to the pre-treatment conditions (Fig. 7b–c), presumably due to decreased transpiration and stomatal control of LE. After partial harvesting, LE also decreased and H slightly increased but the changes were marginal compared to the clear-cut (Fig. 8b–c). Especially in 2016, the Bowen ratio increased as a response to decreasing ET at the partial harvest site (Fig. 8b–c). However, the scaling of H and LE against R_g remained unaltered (Fig. 7b–c). G had a stronger diurnal amplitude and higher daily net heat flux into the soil at the clear-cut than at the tree-covered sites (Fig. 8d), in line with Amiro et al. (2001) and Mamkin et al. (2019). Even at the clear-cut, G still remained an order of magnitude smaller than H and LE. Marginal changes in H and R_n after thinning of a Scots pine stand in southern Finland were also reported by Vesala et al. (2005). The results are also in accordance with Launiainen et al. (2016), who suggested that the sensitivity of boreal forest energy exchange to LAI variations (here created by harvests) is strongest in sparse stands with LAI $< 2\ m^2\ m^{-2}$.

3.3.3. Role of post-treatment vegetation recovery on energy and water balance

Both at the clear-cut and partial harvest sites the changes in LE, GPP and seasonal ET were most pronounced during the first post-treatment year 2016, and partial recovery of these fluxes occurred thereafter (Fig. 8 and Table 5). To explore to which degree the development of field layer vegetation can explain such trends, the model was run for the treated sites with the treatment-specific characteristics (Fig. 2b and Table 1), where the field layer LAI varies according to the range inferred from the post-treatment vegetation inventories. Additionally, the corresponding model outputs for WTL changes in comparison to measurements were evaluated.

At the clear-cut, the observed LE was within the lower end of the model-predicted range (corresponding to small field layer LAI) in 2016, and within its higher end in 2017 and 2018 (corresponding to increased field layer LAI) (Fig. 8c). Thus, we postulate that the rapid establishment of pioneering ground vegetation species and the consequent increase in LAI (Table 1), which enhances plant water use and rainfall interception, is the likely reason for the increasing LE. Model runs with increased field layer LAI also captured the increase in R_n observed at the clear-cut after 2016 (Fig. 8a), which according to the model was a result of decreased surface temperature in response to increased LE, and decreased surface albedo. The role of field layer vegetation establishment is also supported by Fig. 9, where the lower envelope curve representing simulations with high field layer LAI matches the observed WTL changes better in 2017 and 2018. The sensitivity of WTL to field layer LAI at the clear-cut was similar in 2016 and 2017 but much wider during the dry summer 2018 (Fig. 9). The limited effect of field layer LAI on WTL during wet years 2016 and 2017 is because changes in ET are compensated by runoff (Fig. 10b vs. 10d). For example, in 2017 the decrease in field layer LAI results in an ET decrease that is of same magnitude as the increase in runoff, while in 2018 only about half of the ET decrease is compensated by increased runoff. On the other hand, comparison between Fig. 10a and c reveals that at the partial harvest site changes in ET are more directly reflected to WTL because runoff plays a smaller role than at the clear-cut site (Fig. 10b and d).

Contrary to the clear-cut site, the model runs for the partial harvest site with the range of field layer LAI (Table 1) were not able to capture the observed changes during the first post-treatment year 2016. The modelled LE and GPP were overestimated and H underestimated in 2016 (Fig. 8b–c and e), and correspondingly the change in WTL was underestimated (Fig. 9). This indicates that ET and GPP were restricted due to some other phenomenon in 2016. In the model runs, leaf-level photosynthetic and water-use traits of tree and field layer vegetation species were kept constant in time (Table S2), thus omitting possible feedbacks of altered microclimatic conditions and resource competition on leaf physiology. The chlorophyll fluorescence measured from spruce needles, however, showed lower quantum efficiency of PS II (Fv/Fm) at the partial harvest relative to the control site in 2016 (Fig. 11), especially in one-year old needles. Such decrease in Fv/Fm is indicative of a stress response of the photosynthetic apparatus in the shade-adapted spruce undergrowth (e.g., Gnojek, 1992). The needles seemed to adapt rapidly to the altered microclimate, as the difference in Fv/Fm decreased already during the first growing season and leveled out in the

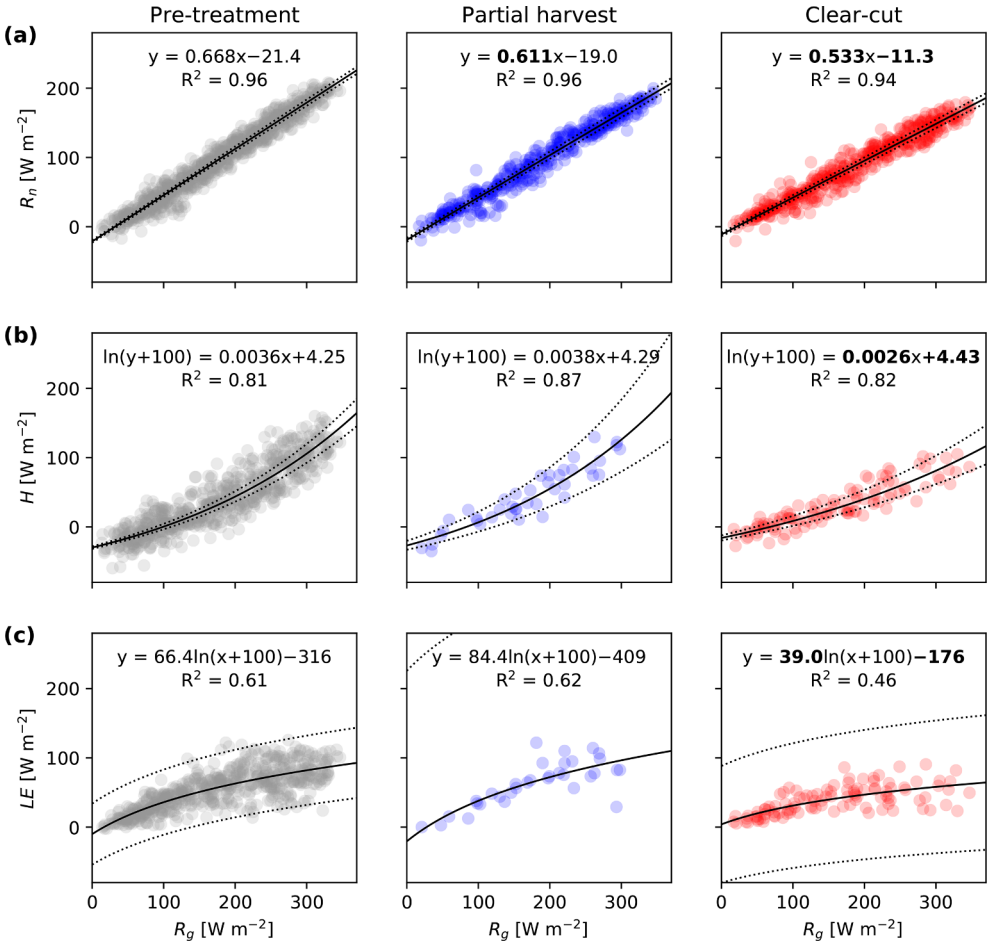

Fig. 7. Dependency of daily measured (a) net radiation, R_n, (b) sensible heat flux, H, and (c) latent heat flux, LE, on global radiation, R_g, during the pre- and post-treatment periods. R^2 denotes the coefficient of determination for the regression curve (least-squares); the regression coefficients differing significantly from pre-treatment values are shown in bold font. Dotted lines show the 95% confidence intervals. To avoid uncertainty induced by gap-filling, only days in May–September with less than 50% of gap-filled observations are included.

second post-treatment year (Fig. 11), which is surprisingly fast (cf. Gnojek, 1992). It is likely that field layer vegetation undergoes a similar stress period, and if leaf marginal water use efficiency (i.e. change of photosynthesis per unit change of transpiration) is not significantly altered after partial harvest, the reduced photosynthetic CO_2 demand of previously shade-adapted vegetation layers will results in lower stomatal conductance and transpiration rate (Medlyn et al., 2011). A stronger reduction in stand transpiration during the first year after forest thinning has also been reported in earlier studies (Bréda et al., 1995; Lagergren et al., 2008).

3.4. Generalizing the role of tree stand in controlling ET and WTL

The nine-year measurements at Lettosuo showed strong seasonal and inter-annual variability in WTL (Figs. 5c and 6a). It is therefore important to disentangle the effect of meteorological variability from harvest responses, something that is seldom possible in empirical studies with a limited number of monitored pre- and post-treatment years. The inter-annual variability in mean growing season WTL, cumulative ET and its components caused by meteorological forcing (2010–2018) and LAI changes were predicted based on model runs. In the simulations, tree stand LAI was set to vary from the non-harvested stand to the clear-cut (Fig. 12) while the species composition was kept constant, i.e. pines, spruces, and birches covered 41%, 35% and 24% of tree stand LAI and their relative LAD profiles were as in Fig. 2a.

This analysis revealed that inter-annual variability of WTL caused by meteorological conditions is much larger than the effect of forest harvesting (Fig. 12a). The role of tree stand LAI on WTL is most pronounced during dry growing seasons, and primarily due to non-linear increase of stand transpiration with LAI (Fig. 12c). During summers with high precipitation and elevated WTL (such as 2014 and 2011), the biological drainage through stand ET has clearly less impact on WTL, resulting into small variations across the simulated LAI range (Fig. 12a). For the same reason, inter-annual variability in WTL decreases with decreasing tree stand LAI (Fig. 12a) and the WTL difference to the control stand varies depending on the year (Fig. 12b). The tree stand volume was shown to have stronger impact on peatland WTL during dry than wet summers also by Sarkkola et al. (2010), meaning that ditch drainage has a more dominant role in the water balance during wet summers.

Depending on the year, the cumulative May–September ET decreased from 294– to 380 mm to 192–229 mm when moving from the non-harvested stand to the clear-cut. This results from the changes in ET components in response to decreasing tree stand LAI (Fig. 12c) (Kozii et al., 2019; Launiainen et al., 2016). First, cumulative rainfall interception responds almost linearly to changes in tree stand LAI

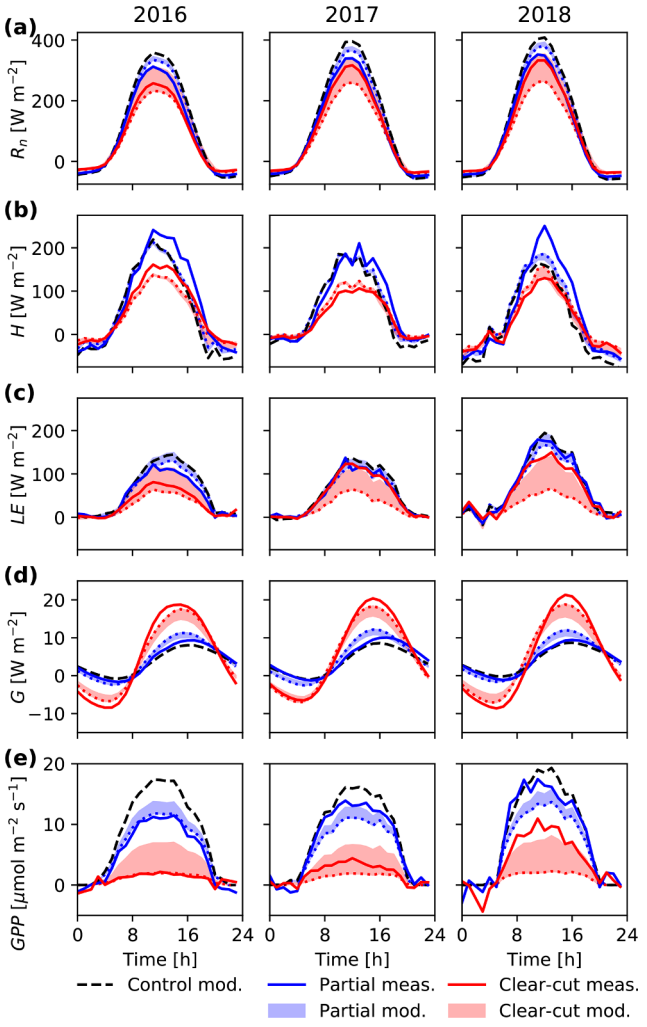

Fig. 8. Measured mean diel cycles at the partial harvest and clear-cut sites during post-treatment growing seasons: (a) net radiation, R_n; (b) sensible heat flux, H; (c) latent heat flux, LE; (d) ground heat flux, G; and (e) gross primary production, GPP. The plotted cycles are based only on such periods during May–September when measurements were available from both sites, excluding periods with > 5.0 mm of rainfall within the past 24 h. The corresponding model predictions for the non-harvested stand (control) are presented as reference, and the shaded areas show the modelled range for the harvested sites when field layer leaf area index is varied as in Table 1. Dotted lines represent model results with low field layer leaf area index.

(Mazza et al., 2011). Second, tree stand transpiration decreases non-linearly and proportionally less than LAI as leaf and tree-level transpiration is enhanced in response to changes in microclimate, increased light availability in particular (Bladon et al., 2006; Bréda et al., 1995; Lagergren and Lindroth, 2004; Launiainen et al., 2016). For Lettosuo, the model suggests spruce transpiration is roughly doubled after opening the overlying canopy in partial harvest. Third, field layer ET and forest floor evaporation increase non-linearly with reduced tree stand LAI as the lower layers become exposed to more light and wind, and higher VPD. This increase in field layer and forest floor ET has a compensating effect on total ET, that in some cases has led to even an increase in total ET after partial harvest (Boczoń et al., 2016).

The WTL change after partial harvest at Lettosuo falls out of the shaded area shown in Fig. 12b because the species composition and vertical LAD profiles were also drastically changed (Fig. 2). Before harvest, Scots pine with conservative water use strategy and thus low transpiration capacity was the dominant species, while after harvest the stand consisted of birch and spruce. This led to a smaller WTL rise at Lettosuo compared to modelled partial harvest in which the LAI of all species was reduced equally (Fig. 12b). The change in species compositions may also explain why our results show smaller WTL rise compared to earlier results on thinning impacts on pure pine stands (Heikurainen and Päivänen, 1970; Päivänen and Sarkkola, 2000).

To further investigate this, model simulations were next made to replicate alternative harvesting strategies: we started from the non-harvested stand as in Fig. 12 but varied the amount and shares of harvested species until reaching clear-cut conditions (Fig. 13). In other words, we altered the species composition as well as the stand structure. The resulting variation in WTL (Fig. 13a) depended mostly on species composition, reflecting the varying transpiration capacity of the tree species, but was also due to the stand structure, which affected the microclimate within the canopy and conditions for forest floor evaporation (Fig. 13c). The removal of dominant pines was associated with the lower end of the WTL range, while removing birches resulted in the greatest WTL rise with decreasing LAI.

In practical forestry, stand volume and basal area are typical metrics to plan harvests, and therefore it is illustrative to consider also the WTL to basal area relationship (Fig. 13b). It differs from the LAI response as allometric relationships, such as diameter to leaf-mass ratio and specific leaf area, vary among species. Partial harvests may in practice be done in several different ways (Nieminen et al., 2018) that may lead to widely varying remaining basal area and LAI. Fig. 13b shows this can lead to a wide range of WTL depending on structure and species composition of the remaining stand. In practical terms, this means that the initial stand heterogeneity and species water use traits can be utilized in harvest planning in order to preserve sufficient ET capacity and biological drainage to control WTL. Favoring mixed stands when possible and, especially, maintaining an admixture of deciduous species with high leaf to basal area ratio and liberal water use strategy (e.g., Lin et al., 2015) could be a cost-effective way to avoid ditch cleaning and also to support biodiversity in peatland forestry. As naturally regenerated undergrowth birches with high transpiration rate per unit leaf area are a typical feature of peatland forests (Sarkkola et al., 2005), retaining such undergrowth in partial harvests should be considered to keep WTL sufficiently low for undisturbed growth of trees with high quality and economical value.

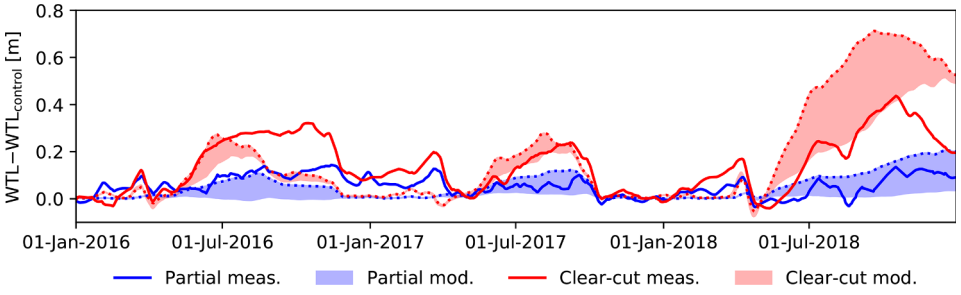

Fig. 9. Mean measured and range of modelled water table level (WTL) difference compared to the control site as 14-day rolling mean during post-treatment years. The shaded areas show the model results when field layer leaf area index is varied as in Table 1 with the dotted line corresponding to the low field layer leaf area index.

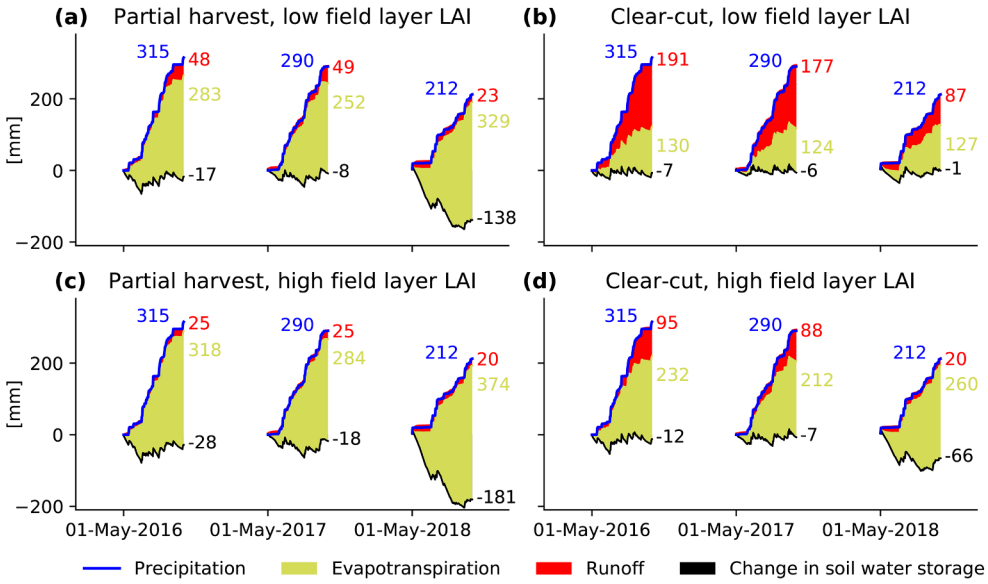

Fig. 10. Cumulative water balance during May–September for the post-treatment period modelled with (a–b) low and (c–d) high field layer leaf area index (LAI) for (a, c) the partial harvest and (b, d) the clear-cut sites. See Table 1 for values of field layer leaf area indices.

4. Conclusions

This study aimed to quantify changes in growing season water balance, WTL and energy fluxes after clear-cutting and partial harvest in a drained boreal peatland forest. To this end, WTL and surface–atmosphere energy and CO_2 exchange were measured at a fertile mixed peatland forest in southern Finland for six pre-treatment and three post-treatment years. The data analysis was accompanied with soil-plant-atmosphere transfer modeling to explore the causal mechanisms behind the observed changes and to disentangle the vegetation controls on water and energy balance from inter-annual meteorological variability. Regarding the three research questions framed in the introduction, our conclusions are as follows:

1) After partial harvest, where 70% of basal area and 50% of LAI was removed, mean growing season WTL rose by only 0.05 m compared to the intact stand, while the response was much greater at the clear-cut site (+0.18 m). R_n, H and LE were significantly reduced and G increased at the clear-cut site, while changes were surprisingly small at the partial harvest site considering the strong reductions in LAI and basal area. The observed changes in energy fluxes were the strongest during the first post-treatment year and partial recovery occurred already during the second year.
2) According to model predictions, the importance of field layer vegetation on ecosystem water and energy fluxes increased after harvests. At the clear-cut, rapid development of field layer vegetation increased ET, and was likely to alter surface albedo and R_n after the first post-treatment year. The model-data comparison and

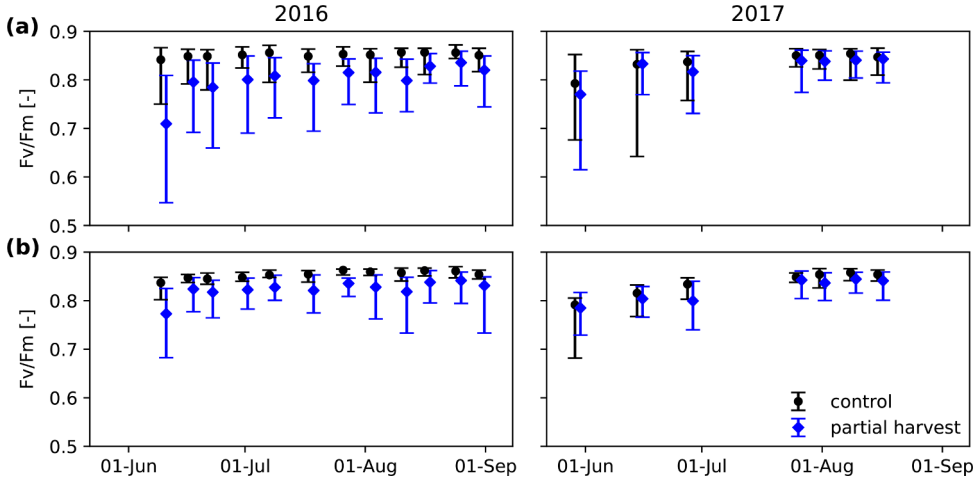

Fig. 11. The chlorophyll fluorescence (Fv/Fm) measured from (a) one-year-old and (b) current-year spruce needles at control and partial harvest sites in 2016 and 2017. Median values and 5…95 percentile ranges are shown as markers and error bars, respectively.

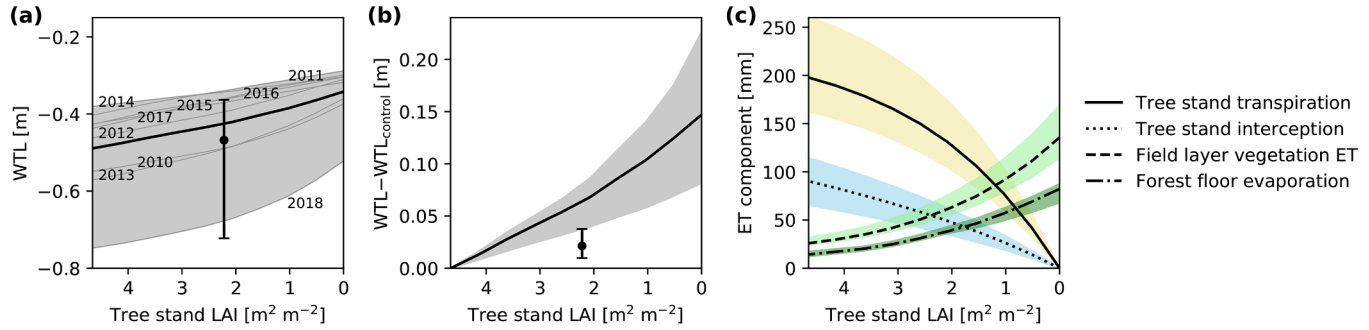

Fig. 12. Modelled (a) mean water table level (WTL), (b) mean WTL difference compared to the non-harvested stand, and (c) cumulative evapotranspiration (ET) components during May–September as a function of tree stand leaf area index (LAI) that is varied from the non-harvested stand (4.66 m^2 m^{-2}, Fig. 2a) to the clear-cut (0 m^2 m^{-2}) while keeping the species composition constant. Markers in panels a and b show model results for the partial harvest stand (LAI = 2.22 m^2 m^{-2}, Fig. 2b). The shaded areas and error bars show the effect of meteorological variability during 2010–2018 (years indicated in panel a), and the lines and dots show the corresponding mean values. LAI of field layer vegetation and surface coverage of moss were fixed to 1.0 m^{2}m^{-2} and 40%, respectively.

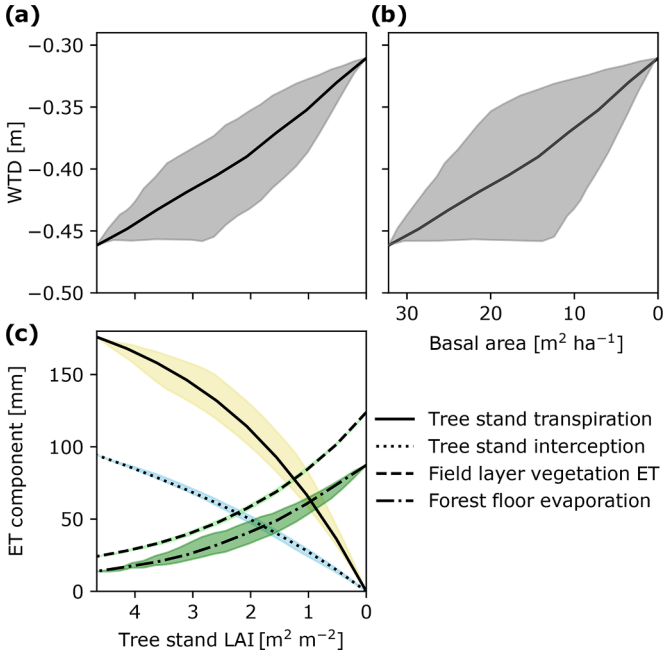

Fig. 13. Modelled (a,b) mean water table level (WTL), and (c) cumulative evapotranspiration (ET) components during May–September 2012 as a function of (a,c) tree stand leaf area index (LAI) and (b) stand basal area, ranging from the non-harvested stand (Fig. 2a) to the clear-cut. The shaded areas show the variability caused by the species composition of the remaining stand, and the lines show the case with the species composition of the initial stand. LAI of field layer vegetation and surface coverage of moss were fixed to 1.0 m^2 m^{-2} and 40%, respectively.

chlorophyll fluorescence measurements suggested that transpiration of the shade-adapted spruce undergrowth was reduced during the first post-treatment growing season due to light-induced stress. However, this was ameliorated already during the second post-treatment year. Better understanding of microclimatic variations, plant stress responses and recovery rates would be an important future research topic for considering the applicability of continuous cover forestry on peatlands.

3) The results indicated that the inter-annual variability in meteorological conditions has a stronger impact on mean growing season WTL than decrease in LAI, reflecting the different roles of ditch drainage vs. ET during wet and dry summers. The WTL response to reduced LAI is non-linear, differs between wet and dry summers, and is sensitive to changes in species composition (water use traits). The non-linearity of WTL and energy exchange in response to changes in LAI or basal area emphasizes that the effect of harvesting depends strongly on initial stand structure. Removing overstory pines but leaving spruces and birches with high transpiration capacity at the partial harvest site explained the small WTL rise observed. This implies that accounting for species composition and vegetation structure in management planning can provide additional control on WTL in peatland forests. Especially, preserving naturally regenerated deciduous undergrowth could limit the WTL rise after partial harvest.

Data availability

Ecosystem flux and meteorological data measured at the central EC mast are available through the ICOS Carbon Portal (10.18160/0jhq-bzmu, ICOS Ecosystem Thematic Centre, 2019). Data for the clear-cut site for two post-treatment years are available through Zenodo (10.5281/zenodo.3384791, Korkiakoski et al., 2019b). WTL and chlorophyll fluorescence data are made available here. The model source code and further data can be obtained from the corresponding author.

Declaration of Competing Interest

The authors declare that they have no known competing financial interests or personal relationships that could have appeared to influence the work reported in this paper.

Acknowledgments

This work was supported by the Academy of Finland projects CCFPeat (no. 310203), CLIMOSS (no. 296116 and 307192), and SOMPA, which was funded by the Strategic Research Council at the Academy of Finland (no. 312912); Kone Foundation; the EU LIFE program through LIFE18 CCM/LV/001158 OrgBalt; the Maj and Tor Nessling foundation; and the Ministry of Transport and Communications through the Integrated Carbon Observing System (ICOS) research. The authors wish to acknowledge CSC – IT Center for Science, Finland, for computational resources. The Finnish Meteorological Institute is acknowledged for their openly available meteorological data (Jokioinen, Somero, Salo Kiikala).

Supplementary materials

Supplementary material associated with this article can be found, in the online version, at doi:10.1016/j.agrformet.2020.108198.

Appendix A. Deriving stand and understory characteristics for model

Leaf area density (LAD) distributions for the main tree species (pine, spruce and birch) were derived using crown shape models, and one-sided leaf area indices (LAI) estimated by an allometric method. First, species specific equations for tree height as a function of DBH (Näslund, 1936) and for trunk base height as a linear function of tree height were determined. This was done using the subset of trees that were measured for trunk base and tree height in addition to DBH. LAI for each tree was then derived based on DBH, trunk base height and tree height using foliage biomass functions (Lehtonen et al., 2020; Tupek et al., 2015) and specific leaf area values (Härkönen et al., 2015). Normalized LAD distributions were derived based on species, tree height and trunk base height (Tahvanainen and Forss, 2008). LAD for each species was obtained as a sum of all individual tree LAD distributions of that species. The LAI and LAD for each species in 2014 and after partial harvest in 2016 are shown in Fig. 2.

Inventory results of field layer vegetation coverage by species and the coverage of moss and litter on the forest floor are shown in Fig. A1. LAI of field layer vegetation was derived by first converting coverage to biomass for each plant type functional group and then total biomass to LAI. Coverage to biomass regressions (Fig. A2a–c) were established from the inventory results of 2009 when field layer vegetation biomass was determined by species in addition to their coverage. In 2018, selected plots in the partial harvest area were measured for vegetation biomass and LAI (Licor LAI-2000) at the same time, which provided a relationship between LAI and biomass (Fig. A2d). Estimated field layer LAI corresponding to each inventory is presented in Fig. A1a. These values were used for model parameterization (see Table 1), however, excluding site VP_{par} because of disturbance caused by proximity of EC mast.

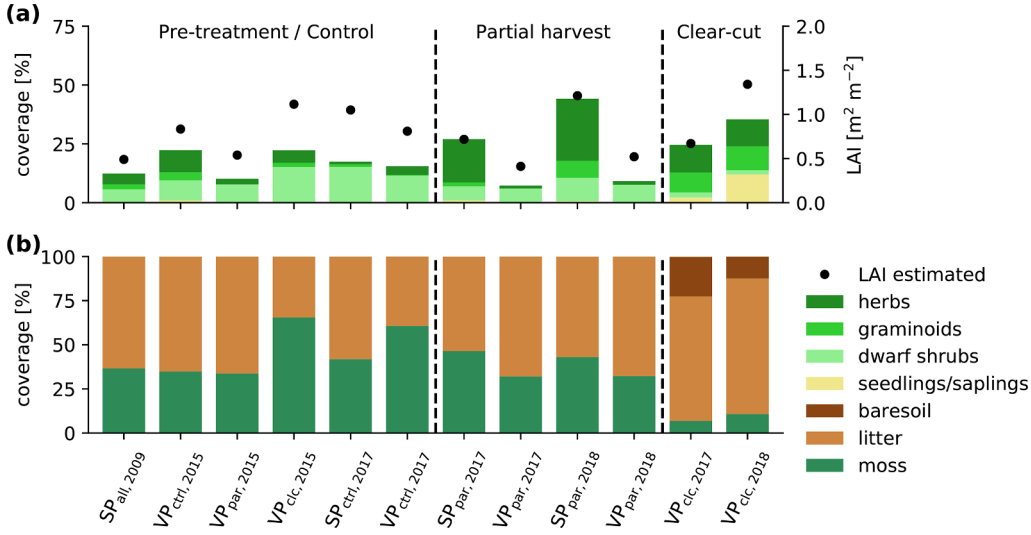

Fig. A1. Results from understory inventories carried out in Lettosuo 2009–2018: (a) projection coverage of field layer vegetation and estimated leaf area index (LAI), and (b) projection coverages of forest floor. SP = stand inventory plots, VP = vegetation inventory plots (see Fig. 1). Subscripts *ctrl, clc* and *par* refer to control, clear-cut and partial harvest areas in Fig. 1 and *all* refers to the whole area.

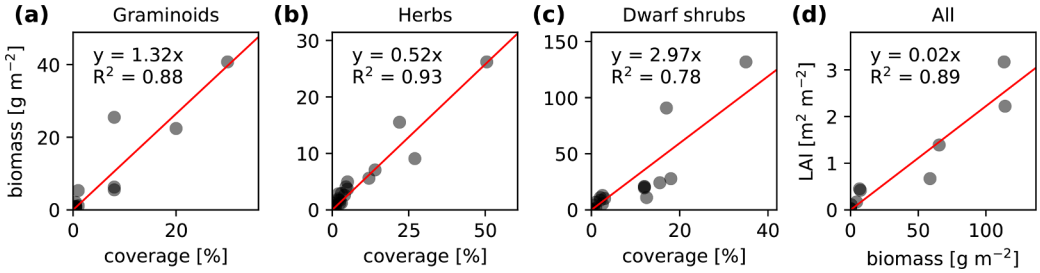

Fig. A2. Relationship between (a–c) field layer vegetation biomass and projection coverage by functional group, and (d) total field layer vegetation leaf area index (LAI) and biomass. R^2 denotes the coefficient of determination for the linear least-squares regression with the intercept forced to zero.

Appendix B. Processing WTL data

WTL was monitored since May 2010 with four automatic loggers and with an additional set of four loggers in each parallel site since 2014–2015 (Fig. 1). The long-term loggers were within the site that was subsequently partially harvested and thus represented partial harvest conditions since March 2016. As WTL measurements were conducted in variable locations (e.g., distance to ditch, local soil hydraulic characteristics, connectivity between pipe and surrounding soil), the data were pre-processed both to discard unreliable measurements and to provide comparable WTL time series for the parallel sites. First, one of the four long-term loggers was discarded due to low correlation with the other loggers and inconsistent dynamics. Linear regressions with a forced slope of unity were then fitted between the remaining three reference time series and the 12 WTL time

series from the transects using the period before the harvesting operations (calibration period). Transect loggers whose average coefficients of determination during the calibration period were < 0.7 when regressed against the reference time series were discarded (5 out of 12). The levels of the remaining 7 WTL time series were corrected to correspond to each of the reference time series based on the fitted regressions. As a result, we obtained a range of WTL for each parallel site, which were comparable to the long-term WTL measurements at the site.

References

Ahti, E., 1987. Water Balance of Drained Peatlands On the Basis of Water Table Simulation During the Snowless Period. Communicationes Instituti Forestalis Fenniae, pp. 141.

Ahti, E., Hökkä, H., 2006. Effects of the growth and volume of Scots pine stands on the level of the water table on peat in central Finland. In: Hydrology and Management of Forested Wetlands, Proceedings of the International Conference, April 8-12, 2006. American Society of Agricultural and Biological Engineers, New Bern, North Carolina, pp. 37.

Alekseychik, P., Mammarella, I., Lindroth, A., Lohila, A., Aurela, M., Laurila, T., Kasurinen, V., Lund, M., Rinne, J., Nilsson, M.B., Peichl, M., Minkkinen, K., Shurpali, N.J., Tuittila, E.S., Martikainen, P.J., Tuovinen, J.P., Vesala, T., 2018. Surface energy exchange in pristine and managed boreal peatlands. Mires Peat 21, 14. https://doi.org/10.19189/MaP.2018.OMB.333.

Amiro, B.D., 2001. Paired-tower measurements of carbon and energy fluxes following disturbance in the boreal forest. Glob. Change Biol. 7, 253–268. https://doi.org/10.1046/j.1365-2486.2001.00398.x.

Arneth, A., Lloyd, J., Shibistova, O., Sogachev, A., Kolle, O., 2006. Spring in the boreal environment: observations on pre-and post-melt energy and CO2 fluxes in two central Siberian ecosystems. Boreal Environ. Res. 11, 311–328.

Aubinet, M., Vesala, T., Papale, D., 2012. Eddy covariance: a Practical Guide to Measurement and Data Analysis. Springer Science & Business Media.

Banerjee, T., Linn, R., 2018. Effect of vertical canopy architecture on transpiration, thermoregulation and carbon assimilation. Forests 9, 198. https://doi.org/10.3390/f9040198.

Berglund, Ö., Berglund, K., 2011. Influence of water table level and soil properties on emissions of greenhouse gases from cultivated peat soil. Soil Biol. Biochem. 43, 923–931. https://doi.org/10.1016/j.soilbio.2011.01.002.

Bergstedt, J., Milberg, P., 2001. The impact of logging intensity on field-layer vegetation in Swedish boreal forests. For. Ecol. Manag. 154, 105–115. https://doi.org/10.1016/S0378-1127(00)00642-3.

Bladon, K.D., Silins, U., Landhäusser, S.M., Lieffers, V.J., 2006. Differential transpiration by three boreal tree species in response to increased evaporative demand after variable retention harvesting. Agric. For. Meteorol. 138, 104–119. https://doi.org/10.1016/j.agrformet.2006.03.015.

Boczoń, A., Dudzińska, M., Kowalska, A., 2016. Effect of thinning on evaporation of Scots pine forest. Appl. Ecol. Environ. Res. 14, 367–379.

Bowden, J.D., Bauerle, W.L., 2008. Measuring and modeling the variation in species-specific transpiration in temperate deciduous hardwoods. Tree Physiol 28, 1675–1683. https://doi.org/10.1093/treephys/28.11.1675.

Bréda, N., Granier, A., Aussenac, G., 1995. Effects of thinning on soil and tree water relations, transpiration and growth in an oak forest (Quercus petraea (Matt.) Liebl.). Tree Physiol 15, 295–306. https://doi.org/10.1093/treephys/15.5.295.

Dubé, S., Plamondon, A.P., Rothwell, R.L., 1995. Watering up after clear-cutting on forested wetlands of the St. Lawrence lowland. Water Resour. Res. 31, 1741–1750. https://doi.org/10.1029/95WR00427.

Farquhar, G.D., Caemmerer, S.V., Berry, J.A., 1980. A biochemical model for photosynthetic CO2 assimulation in leaves of C3 species. Planta 149, 78–90. https://doi.org/10.1007/BF00386231.

Foken, Th., Wichura, B., 1996. Tools for quality assessment of surface-based flux measurements. Agric. For. Meteorol. 78, 83–105. https://doi.org/10.1016/0168-1923(95)02248-1.

Gebauer, R., Volařík, D., Urban, J., Børja, I., Nagy, N.E., Eldhuset, T.D., Krokene, P., 2011. Effect of thinning on anatomical adaptations of Norway spruce needles. Tree Physiol 31, 1103–1113. https://doi.org/10.1093/treephys/tpr081.

Gebhardt, T., Häberle, K.-H., Matyssek, R., Schulz, C., Ammer, C., 2014. The more, the better? Water relations of Norway spruce stands after progressive thinning. Agric. For. Meteorol. 197, 235–243. https://doi.org/10.1016/j.agrformet.2014.05.013.

Gnojek, A.R., 1992. Changes in chlorophyll fluorescence and chlorophyll content in suppressed Norway spruce [Picea abies (L.) Karst.] in response to release cutting. Trees 6, 41–47. https://doi.org/10.1007/BF00224498.

Goodrich, J.P., Oechel, W.C., Gioli, B., Moreaux, V., Murphy, P.C., Burba, G., Zona, D., 2016. Impact of different eddy covariance sensors, site set-up, and maintenance on the annual balance of CO2 and CH4 in the harsh Arctic environment. Agric. For. Meteorol. 228–229, 239–251. https://doi.org/10.1016/j.agrformet.2016.07.008.

Grelle, A., Lundberg, A., Lindroth, A., Morén, A.-S., Cienciala, E., 1997. Evaporation components of a boreal forest: variations during the growing season. J. Hydrol. 197, 70–87. https://doi.org/10.1016/S0022-1694(96)03267-2.

Hamberg, L., Hotanen, J.-P., Nousiainen, H., Nieminen, T.M., Ukonmaanaho, L., 2019. Recovery of understorey vegetation after stem-only and whole-tree harvesting in drained peatland forests. For. Ecol. Manag. 442, 124–134. https://doi.org/10.1016/j.foreco.2019.04.002.

Hämet-Ahti, L., Suominen, J., Ulvinen, T., Uotila, P., 1998. Field Flora of Finland. 4th ed. Finnish Museum of Natural History, Botanical Museum, Helsinki.

Hånell, B., 1988. Postdrainage forest productivity of peatlands in Sweden. Can. J. For. Res. 18, 1443–1456. https://doi.org/10.1139/x88-223.

Hannerz, M., Hånell, B., 1993. Changes in the vascular plant vegetation after different cutting regimes on a productive Peatland site in Central Sweden. Scand. J. For. Res. 8, 193–203. https://doi.org/10.1080/02827589309382769.

Härkönen, S., Lehtonen, A., Manninen, T., Tuominen, S., Peltoniemi, M., 2015. Estimating forest leaf area index using satellite images: comparison of k-NN based Landsat-NFI LAI with MODIS-RSR based LAI product for Finland. Boreal Environ. Res. 20.

Heikurainen, L., 1967. Influence of cuttings on the water economy of drained peatlands. Acta For. Fenn. 82, 1–45. https://doi.org/10.14214/aff.7175.

Heikurainen, L., Päivänen, J., 1970. The effect of thinning, clear cutting and fertilization on the hydrology of peatland drained for forestry. Acta For. Fenn. 104. https://doi.org/10.14214/aff.7538.

Hökkä, H., Koivusalo, H., Ahti, E., Nieminen, M., Laine, J., Saarinen, M., Lauren, A., Alm, J., Nikinmaa, E., Klöve, B., 2008a. Effects of tree stand transpiration and interception on site water balance in drained peatlands: experimental design and measurements. In: International Peat Congress, pp. 169–171.

Hökkä, H., Repola, J., Laine, J., 2008b. Quantifying the interrelationship between tree stand growth rate and water table level in drained peatland sites within Central Finland. Can. J. For. Res. 38, 1775–1783. https://doi.org/10.1139/X08-028.

Holden, J., 2006. Peatland hydrology. Dev. Earth Surf. Process 9, 319–346.

Holden, J., Evans, M.G., Burt, T.P., Horton, M., 2006. Impact of land drainage on peatland hydrology. J Env. Qual 35, 1764–1778. https://doi.org/10.2134/jeq2005.0477.

Hooghoudt, S.B., 1940. General consideration of the problem of field drainage by parallel drains, ditches, watercourses, and channels. Publ. No. 7. In: Contribution to the Knowledge of Some Physical Parameters of the Soil. Bodemkundig Instituut, Groningen, The Netherlands.

ICOS Ecosystem Thematic Centre, 2019. Drought-2018 ecosystem eddy covariance flux product from Lettosuo (Version 1.0) [Data set]. 10.18160/0jhq-bzmu.

Joensuu, S., Ahti, E., Vuollekoski, M., 1999. The effects of peatland forest ditch maintenance on suspended solids in runoff. Boreal Env. Res 4, 343–356.

Jutras, S., Plamondon, A.P., 2005. Water table rise after harvesting in a treed fen previously drained for forestry. Suo 56, 95–100.

Juutinen, A., Ahtikoski, A., Mäkipää, R., Shanin, V., 2018. Effect of harvest interval and intensity on the profitability of uneven-aged management of Norway spruce stands. For. Int. J. For. Res. 91, 589–602. https://doi.org/10.1093/forestry/cpy018.

Kaila, A., Laurén, A., Sarkkola, S., Koivusalo, H., Ukonmaanaho, L., O'Driscoll, C., Xiao, L., Asam, Z., Nieminen, M., 2015. Effect of clear-felling and harvest residue removal on nitrogen and phosphorus export from drained Norway spruce mires in southern Finland. Boreal Environ. Res. 20.

Kaila, A., Sarkkola, S., Laurén, A., Ukonmaanaho, L., Koivusalo, H., Xiao, L., O'Driscoll, C., Tervahauta, A., Nieminen, M., 2014. Phosphorus export from drained Scots pine mires after clear-felling and bioenergy harvesting. For. Ecol. Manag. 325, 99–107. https://doi.org/10.1016/j.foreco.2014.03.025.

Kang, M., Kim, J., Malla Thakuri, B., Chun, J., Cho, C., 2018. New gap-filling and partitioning technique for H_2O eddy fluxes measured over forests. Biogeosciences 15, 631–647. https://doi.org/10.5194/bg-15-631-2018.

Katul, G., Manzoni, S., Palmroth, S., Oren, R., 2010. A stomatal optimization theory to describe the effects of atmospheric CO2 on leaf photosynthesis and transpiration. Ann. Bot. 105, 431–442. https://doi.org/10.1093/aob/mcp292.

Kieloaho, A.-J., Launianen, S., 2018. Effects of functional traits of bryophyte layer on water cycling and energy balance in boreal and arctic ecosystems. In: EGU General Assembly Conference Abstracts, pp. 11786.

Koivusalo, H., Heikinheimo, M., Karvonen, T., 2001. Test of a simple two-layer parameterisation to simulate the energy balance and temperature of a snow pack. Theor. Appl. Climatol. 70, 65–79. https://doi.org/10.1007/s007040170006.

Kojola, S., Penttila, T., Laiho, R., 2004. Impacts of different thinning regimes on the yield of uneven-structured Scots pine stands on drained peatlands. Silva Fenn 38, 393–403. https://doi.org/10.14214/sf.407.

Kolari, P., Lappalainen, H.K., Hänninen, H., Hari, P., 2007. Relationship between temperature and the seasonal course of photosynthesis in Scots pine at northern timberline and in southern boreal zone. Tellus Ser. B-Chem. Phys. Meteorol. 59, 542–552. https://doi.org/10.1111/j.1600-0889.2007.00262.x.

Korkiakoski, M., Tuovinen, J.-P., Penttilä, T., Sarkkola, S., Ojanen, P., Minkkinen, K., Rainne, J., Laurila, T., Lohila, A., 2019a. Greenhouse gas and energy fluxes in a boreal peatland forest after clear-cutting. Biogeosciences 16, 3703–3723. https://doi.org/10.5194/bg-16-3703-2019.

Korkiakoski, M., Tuovinen, J.-P., Penttilä, T., Sarkkola, S., Ojanen, P., Minkkinen, K., Rainne, J., Laurila, T., Lohila, A., 2019b. Greenhouse gas and energy fluxes in a boreal peatland forest after clearcutting [Data set]. 10.5281/zenodo.3384791.

Kormann, R., Meixner, F.X., 2001. An Analytical Footprint Model For Non-Neutral Stratification. Bound.-Layer Meteorol. 99, 207–224. https://doi.org/10.1023/A:1018991015119.

Koskinen, M., Sallantaus, T., Vasander, H., 2011. Post-restoration development of organic carbon and nutrient leaching from two ecohydrologically different peatland sites. Ecol. Eng., Biogeochemical aspects of ecosystem restoration and rehabilitation 37, 1008–1016. https://doi.org/10.1016/j.ecoleng.2010.06.036.

Kozii, N., Haahti, K., Tor-ngern, P., Chi, J., Hasselquist, E.M., Laudon, H., Launiainen, S., Oren, R., Peichl, M., Wallerman, J., Hasselquist, N.J., 2019. Partitioning the forest water balance within a boreal catchment using sapflux, eddy covariance and process-

based model. Hydrol. Earth Syst. Sci. Discuss. 1–50. https://doi.org/10.5194/hess-2019-541.
Kuusinen, N., Tomppo, E., Shuai, Y., Berninger, F., 2014. Effects of forest age on albedo in boreal forests estimated from MODIS and Landsat albedo retrievals. Remote Sens. Environ. 145, 145–153. https://doi.org/10.1016/j.rse.2014.02.005.
Lagergren, F., Lankreijer, H., Kučera, J., Cienciala, E., Mölder, M., Lindroth, A., 2008. Thinning effects on pine-spruce forest transpiration in central Sweden. For. Ecol. Manag., Large-scale experimentation and oak regeneration 255, 2312–2323. https://doi.org/10.1016/j.foreco.2007.12.047.
Lagergren, F., Lindroth, A., 2004. Variation in sapflow and stem growth in relation to tree size, competition and thinning in a mixed forest of pine and spruce in Sweden. For. Ecol. Manag. 188, 51–63. https://doi.org/10.1016/j.foreco.2003.07.018.
Launiainen, S., 2010. Seasonal and inter-annual variability of energy exchange above a boreal Scots pine forest. Biogeosciences 7, 3921–3940. https://doi.org/10.5194/bg-7-3921-2010.
Launiainen, S., Guan, M., Salmivaara, A., Kieloaho, A.-J., 2019. Modeling boreal forest evapotranspiration and water balance at stand and catchment scales: a spatial approach. Hydrol. Earth Syst. Sci. 23. https://doi.org/10.5194/hess-23-3457-2019.
Launiainen, S., Katul, G.G., Kolari, P., Lindroth, A., Lohila, A., Aurela, M., Varlagin, A., Grelle, A., Vesala, T., 2016. Do the energy fluxes and surface conductance of boreal coniferous forests in Europe scale with leaf area? Glob. Change Biol 22, 4096–4113. https://doi.org/10.1111/gcb.13497.
Launiainen, S., Katul, G.G., Kolari, P., Vesala, T., Hari, P., 2011. Empirical and optimal stomatal controls on leaf and ecosystem level CO2 and H2O exchange rates. Agric. For. Meteorol. 151, 1672–1689. https://doi.org/10.1016/j.agrformet.2011.07.001.
Launiainen, S., Katul, G.G., Lauren, A., Kolari, P., 2015. Coupling boreal forest CO2, H2O and energy flows by a vertically structured forest canopy – Soil model with separate bryophyte layer. Ecol. Model. 312, 385–405. https://doi.org/10.1016/j.ecolmodel.2015.06.007.
Lehtonen, A., Heikkinen, J., Petersson, H., Ťupek, B., Liski, E., Mäkelä, A., 2020. Scots pine and Norway spruce foliage biomass in Finland and Sweden — Testing traditional models vs. the pipe model theory. Can. J. For. Res. 50, 146–154. https://doi.org/10.1139/cjfr-2019-0211.
Leuning, R., van Gorsel, E., Massman, W.J., Isaac, P.R., 2012. Reflections on the surface energy imbalance problem. Agric. For. Meteorol. 156, 65–74. https://doi.org/10.1016/j.agrformet.2011.12.002.
Lin, Y.-S., Medlyn, B.E., Duursma, R.A., Prentice, I.C., Wang, H., Baig, S., Eamus, D., de Dios, V.R., Mitchell, P., Ellsworth, D.S., de Beeck, M.O., Wallin, G., Uddling, J., Tarvainen, L., Linderson, M.-L., Cernusak, L.A., Nippert, J.B., Ocheltree, T.W., Tissue, D.T., Martin-StPaul, N.K., Rogers, A., Warren, J.M., De Angelis, P., Hikosaka, K., Han, Q., Onoda, Y., Gimeno, T.E., Barton, C.V.M., Bennie, J., Bonal, D., Bosc, A., Löw, M., Macinins-Ng, C., Rey, A., Rowland, L., Setterfield, S.A., Tausz-Posch, S., Zaragoza-Castells, J., Broadmeadow, M.S.J., Drake, J.E., Freeman, M., Ghannoum, O., Hutley, L.B., Kelly, J.W., Kikuzawa, K., Kolari, P., Koyama, K., Limousin, J.-M., Meir, P., Lola da Costa, A.C., Mikkelsen, T.N., Salinas, N., Sun, W., Wingate, L., 2015. Optimal stomatal behaviour around the world. Nat. Clim. Change 5, 459–464. https://doi.org/10.1038/nclimate2550.
Lukeš, P., Stenberg, P., Rautiainen, M., 2013. Relationship between forest density and albedo in the boreal zone. Ecol. Model. 261–262, 74–79. https://doi.org/10.1016/j.ecolmodel.2013.04.009.
Mäkiranta, P., Riutta, T., Penttilä, T., Minkkinen, K., 2010. Dynamics of net ecosystem CO2 exchange and heterotrophic soil respiration following clearfelling in a drained peatland forest. Agric. For. Meteorol. 150, 1585–1596. https://doi.org/10.1016/j.agrformet.2010.08.010.
Malhotra, A., Roulet, N.T., Wilson, P., Giroux-Bougard, X., Harris, L.I., 2016. Ecohydrological feedbacks in peatlands: an empirical test of the relationship among vegetation, microtopography and water table. Ecohydrology 9, 1346–1357. https://doi.org/10.1002/eco.1731.
Mamkin, V., Kurbatova, J., Avilov, V., Ivanov, D., Kuricheva, O., Varlagin, A., Yaseneva, I., Olchev, A., 2019. Energy and CO2 exchange in an undisturbed spruce forest and clear-cut in the Southern Taiga. Agric. For. Meteorol. 265, 252–268. https://doi.org/10.1016/j.agrformet.2018.11.018.
Martikainen, P.J., Nykänen, H., Crill, P., Silvola, J., 1993. Effect of a lowered water table on nitrous oxide fluxes from northern peatlands. Nature 366, 51.
Mazza, G., Amorini, E., Cutini, A., Manetti, M.C., 2011. The influence of thinning on rainfall interception by Pinus pinea L. in Mediterranean coastal stands (Castel Fusano—Rome). Ann. For. Sci. 68, 1323–1332. https://doi.org/10.1007/s13595-011-0142-7.
McCaughey, J.H., 1981. Impact of Clearcutting of Coniferous Forest on the Surface Radiation Balance. J. Appl. Ecol. 18, 815–826. https://doi.org/10.2307/2402372.
McMillen, R.T., 1988. An eddy correlation technique with extended applicability to non-simple terrain. Bound.-Layer Meteorol. 43, 231–245. https://doi.org/10.1007/BF00128405.
McNaughton, K.G., Jarvis, P.G., 1983. Predicting effects of vegetation changes on transpiration and evaporation. Water Deficits Plant Growth 7, 1–47.
Medlyn, B.E., Duursma, R.A., Eamus, D., Ellsworth, D.S., Prentice, I.C., Barton, C.V.M., Crous, K.Y., Angelis, P.D., Freeman, M., Wingate, L., 2011. Reconciling the optimal and empirical approaches to modelling stomatal conductance. Glob. Change Biol. 17, 2134–2144. https://doi.org/10.1111/j.1365-2486.2010.02375.x.
Minkkinen, K., Ojanen, P., Penttilä, T., Aurela, M., Laurila, T., Tuovinen, J.-P., Lohila, A., 2018. Persistent carbon sink at a boreal drained bog forest. Biogeosciences 15, 3603–3624. https://doi.org/10.5194/bg-15-3603-2018.
Moore, C.J., 1986. Frequency response corrections for eddy correlation systems. Bound.-Layer Meteorol. 37, 17–35. https://doi.org/10.1007/BF00122754.
Moore, T.R., Knowles, R., 1989. The Influence of Water Table Levels on Methane and Carbon Dioxide Emissions from Peatland Soils. Can. J. Soil Sci. 69, 33–38. https://doi.org/10.4141/cjss89-004.
Murchie, E.H., Lawson, T., 2013. Chlorophyll fluorescence analysis: a guide to good practice and understanding some new applications. J. Exp. Bot. 64, 3983–3998. https://doi.org/10.1093/jxb/ert208.
Musarika, S., Atherton, C.E., Gomersall, T., Wells, M.J., Kaduk, J., Cumming, A.M.J., Page, S.E., Oechel, W.C., Zona, D., 2017. Effect of water table management and elevated CO2 on radish productivity and on CH4 and CO2 fluxes from peatlands converted to agriculture. Sci. Total Environ. 584–585, 665–672. https://doi.org/10.1016/j.scitotenv.2017.01.094.
Näslund, M., 1936. Skogsförsöksanstaltens Gallringsförsök I Tallskog (Report). Stockholm.
Nieminen, M., 2003. Effects of clear-cutting and site preparation on water quality from a drained Scots pine mire in southern Finland. Boreal Environ. Res. 8, 53–59.
Nieminen, M., Ahti, E., Koivusalo, H., Mattsson, T., Sarkkola, S., Laurén, A., 2010. Export of suspended solids and dissolved elements from peatland areas after ditch network maintenance in South-Central Finland. Silva Fenn 44, 39–49. https://doi.org/10.14214/sf.161.
Nieminen, M., Hökkä, H., Laiho, R., Juutinen, A., Ahtikoski, A., Pearson, M., Kojola, S., Sarkkola, S., Launiainen, S., Valkonen, S., Penttilä, T., Lohila, A., Saarinen, M., Haahti, K., Mäkipää, R., Miettinen, J., Ollikainen, M., 2018. Could continuous cover forestry be an economically and environmentally feasible management option on drained boreal peatlands? For. Ecol. Manag. 424, 78–84. https://doi.org/10.1016/j.foreco.2018.04.046.
Nieminen, M., Koskinen, M., Sarkkola, S., Laurén, A., Kaila, A., Kiikkilä, O., Nieminen, T.M., Ukonmaanaho, L., 2015. Dissolved organic carbon export from harvested peatland forests with differing site characteristics. Water. Air. Soil Pollut. 226, 181. https://doi.org/10.1007/s11270-015-2444-0.
Ojanen, P., Minkkinen, K., 2019. The dependence of net soil CO2 emissions on water table depth in boreal peatlands drained for forestry. Mires Peat 24. https://doi.org/10.19189/MaP.2019.OMB.StA.1751.
Ojanen, P., Minkkinen, K., Alm, J., Penttilä, T., 2010. Soil–atmosphere CO2, CH4 and N2O fluxes in boreal forestry-drained peatlands. For. Ecol. Manag. 260, 411–421. https://doi.org/10.1016/j.foreco.2010.04.036.
Ojanen, P., Minkkinen, K., Penttilä, T., 2013. The current greenhouse gas impact of forestry-drained boreal peatlands. For. Ecol. Manag. 289, 201–208. https://doi.org/10.1016/j.foreco.2012.10.008.
Päivänen, J., 1973. Hydraulic conductivity and water retention in peat soils. Acta Fenn 129, 1–70. https://doi.org/10.14214/aff.7563.
Päivänen, J., Hånell, B., 2012. Peatland Ecology and Forestry – a Sound Approach. University of Helsinki Department of Forest Sciences Publication 3, Helsinki, Finland.
Päivänen, J., Sarkkola, S., 2000. The effect of thinning and ditch network maintenance on the water table level in a Scots pine stand on peat soil. Suo 51, 131–138.
Pirinen, P., Simola, H., Aalto, J., Kaukoranta, J.-P., Karlsson, P., Ruuhela, R., 2012. Tilastoja Suomen ilmastosta 1981–2010 (Climatological statistics of Finland 1981-2010).
Pommerening, A., Murphy, S.T., 2004. A review of the history, definitions and methods of continuous cover forestry with special attention to afforestation and restocking. For. Int. J. For. Res. 77, 27–44. https://doi.org/10.1093/forestry/77.1.27.
Préfontaine, G., Jutras, S., 2017. Variation in stand density, black spruce individual growth and plant community following 20years of drainage in post-harvest boreal peatlands. For. Ecol. Manag. 400, 321–331. https://doi.org/10.1016/j.foreco.2017.06.029.
Rannik, Ü., Altimir, N., Raittila, J., Suni, T., Gaman, A., Hussein, T., Hölttä, T., Lassila, H., Latokartano, M., Lauri, A., Natsheh, A., Petäjä, T., Sorjamaa, R., Ylä-Mella, H., Keronen, P., Berninger, F., Vesala, T., Hari, P., Kulmala, M., 2002. Fluxes of carbon dioxide and water vapour over Scots pine forest and clearing. Agric. For. Meteorol. 111, 187–202. https://doi.org/10.1016/S0168-1923(02)00022-9.
Regina, K., Sheehy, J., Myllys, M., 2015. Mitigating greenhouse gas fluxes from cultivated organic soils with raised water table. Mitig. Adapt. Strateg. Glob. Change 20, 1529–1544. https://doi.org/10.1007/s11027-014-9559-2.
Renger, M., Wessolek, G., Schwärzel, K., Sauerbrey, R., Siewert, C., 2002. Aspects of peat conservation and water management. J. Plant Nutr. Soil Sci. 165, 487–493 10.1002/1522-2624(200208)165:4<487::AID-JPLN487>3.0.CO;2-C.
Sarkkola, S., Alenius, V., Hökkä, H., Laiho, R., Päivänen, J., Penttilä, T., 2003. Changes in structural inequality in Norway spruce stands on peatland sites after water-level drawdown. Can. J. For. Res. 33, 222–231. https://doi.org/10.1139/x02-179.
Sarkkola, S., Hökkä, H., Koivusalo, H., Nieminen, M., Ahti, E., Päivänen, J., Laine, J., 2010. Role of tree stand evapotranspiration in maintaining satisfactory drainage conditions in drained peatlands. Can J For. Res 40, 1485–1496. https://doi.org/10.1139/X10-084.
Sarkkola, S., Hökkä, H., Laiho, R., Päivänen, J., Penttilä, T., 2005. Stand structural dynamics on drained peatlands dominated by Scots pine. For. Ecol. Manag. 206, 135–152. https://doi.org/10.1016/j.foreco.2004.10.064.
Sarkkola, S., Nieminen, M., Koivusalo, H., Laurén, A., Ahti, E., Launiainen, S., Nikinmaa, E., Marttila, H., Laine, J., Hökkä, H., 2013. Domination of growing-season evapotranspiration over runoff makes ditch network maintenance in mature peatland forests questionable. Mires Peat 11, 1–11.
Sikström, U., Hökkä, H., 2016. Interactions between soil water conditions and forest stands in boreal forests with implications for ditch network maintenance. Silva Fenn. 50. https://doi.org/10.14214/sf.1416.
Simonin, K., Kolb, T.E., Montes-Helu, M., Koch, G.W., 2007. The influence of thinning on components of stand water balance in a ponderosa pine forest stand during and after extreme drought. Agric. For. Meteorol. 143, 266–276. https://doi.org/10.1016/j.agrformet.2007.01.003.
Song, C., Katul, G., Oren, R., Band, L.E., Tague, C.L., Stoy, P.C., McCarthy, H.R., 2009. Energy, water, and carbon fluxes in a loblolly pine stand: results from uniform and

gappy canopy models with comparisons to eddy flux data. J. Geophys. Res.-Biogeosciences 114, G04021. https://doi.org/10.1029/2009JG000951.
Tahvanainen, T., Forss, E., 2008. Individual tree models for the crown biomass distribution of Scots pine, Norway spruce and birch in Finland. For. Ecol. Manag. 255, 455–467. https://doi.org/10.1016/j.foreco.2007.09.035.
Tahvonen, O., 2016. Economics of rotation and thinning revisited: the optimality of clearcuts versus continuous cover forestry. For. Policy Econ. 62, 88–94. https://doi.org/10.1016/j.forpol.2015.08.013.
Tupek, B., Mäkipää, R., Heikkinen, J., Peltoniemi, M., Ukonmaanaho, L., Hokkanen, T., Nöjd, P., Nevalainen, S., Lindgren, M., Lehtonen, A., 2015. Foliar turnover rates in Finland-comparing estimates from needle-cohort and litterfall-biomass methods. Boreal Environ. Res. 22.
Ulvinen, T., Syrjänen, K., Anttila, S., 2002. Bryophytes of Finland—Distribution, ecology and red list status (in Finnish). Suom. Ymp. Hels. 353.
Van Dam, J.C., Feddes, R.A., 2000. Numerical simulation of infiltration, evaporation and shallow groundwater levels with the Richards equation. J. Hydrol. 233, 72–85. https://doi.org/10.1016/S0022-1694(00)00227-4.
van Dijk, A.I.J.M., Gash, J.H., van Gorsel, E., Blanken, P.D., Cescatti, A., Emmel, C., Gielen, B., Harman, I.N., Kiely, G., Merbold, L., Montagnani, L., Moors, E., Sottocornola, M., Varlagin, A., Williams, C.A., Wohlfahrt, G., 2015. Rainfall interception and the coupled surface water and energy balance. Agric. For. Meteorol. 214–215, 402–415. https://doi.org/10.1016/j.agrformet.2015.09.006.
Vesala, T., Suni, T., Rannik, Ü., Keronen, P., Markkanen, T., Sevanto, S., Grönholm, T., Smolander, S., Kulmala, M., Ilvesniemi, H., Ojansuu, R., Uotila, A., Levula, J., Mäkelä, A., Pumpanen, J., Kolari, P., Kulmala, L., Altimir, N., Berninger, F., Nikinmaa, E., Hari, P., 2005. Effect of thinning on surface fluxes in a boreal forest. Glob. Biogeochem. Cycles 19. https://doi.org/10.1029/2004GB002316.
von Post, L., 1922. Sveriges Geologiska Undersöknings torvinventering och n\a agra av dess hittills vunna resultat. Sven. Mosskulturforeningens Tidskr. 1–37.
Waddington, J.M., Morris, P.J., Kettridge, N., Granath, G., Thompson, D.K., Moore, P.A., 2015. Hydrological feedbacks in northern peatlands. Ecohydrology 8, 113–127. https://doi.org/10.1002/eco.1493.
Watanabe, T., Mizutani, K., 1996. Model study on micrometeorological aspects of rainfall interception over an evergreen broad-leaved forest. Agric. For. Meteorol. 80, 195–214. https://doi.org/10.1016/0168-1923(95)02301-1.
Webb, E.K., Pearman, G.I., Leuning, R., 1980. Correction of flux measurements for density effects due to heat and water vapour transfer. Q. J. R. Meteorol. Soc. 106, 85–100. https://doi.org/10.1002/qj.49710644707.
Weltzin, J.F., Bridgham, S.D., Pastor, J., Chen, J., Harth, C., 2003. Potential effects of warming and drying on peatland plant community composition. Glob. Change Biol. 9, 141–151. https://doi.org/10.1046/j.1365-2486.2003.00571.x.
Westman, C.J., Laiho, R., 2003. Nutrient dynamics of drained peatland forests. Biogeochemistry 63, 269–298. https://doi.org/10.1023/A:1023348806857.
Wutzler, T., Lucas-Moffat, A., Migliavacca, M., Knauer, J., Sickel, K., Šigut, L., Menzer, O., Reichstein, M., 2018. Basic and extensible post-processing of eddy covariance flux data with REddyProc. Biogeosciences 15, 5015–5030. https://doi.org/10.5194/bg-15-5015-2018.
Zhao, W., Qualls, R.J., 2006. Modeling of long-wave and net radiation energy distribution within a homogeneous plant canopy via multiple scattering processes. Water Resour. Res. 42. https://doi.org/10.1029/2005WR004581.
Zhao, W.G., Qualls, R.J., 2005. A multiple-layer canopy scattering model to simulate shortwave radiation distribution within a homogeneous plant canopy. Water Resour. Res. 41, A08409. https://doi.org/10.1029/2005WR004016.